Norges miljø- og biovitenskapelige universitet

Master's Thesis 2016 60 ECTS
Department of Chemistry, Biotechnology and Food Science

Investigation of the WNT and AKT/mTOR Signaling Pathways in Early Differentiation of Embryonic Stem Cells

Sigrid Aslaksen
Master of Biotechnology and Biochemistry

Acknowledgements

First I would like to thank my supervisor Stefan Krauss for the opportunity to do my thesis research in his research group. Stefan has given me full support and has shown a great willingness to pursue any question that has arisen during my thesis work. I am also incredibly grateful for all the theoretical knowledge he has shared.

Thank you also to my co-supervisor Jo Waaler who has been inspiring and helping me in undertaking this project. I am very grateful for his constant positive energy, enthusiasm, encouragement and curiosity regarding my topic. I would also like to express my gratitude to my internal supervisor Tor Erling Lea for his guidance and interest for bringing this master thesis to a successful end.

I also want to thank all my colleagues for all the support, discussion and communication, among them Gareth, Rich, Santosh, Petter, Nina, Line, Kaja, Shoshy, Max, Kristina, Frøydis, Camilla, Tore, Steven, Hanne and Dorna.

Finally, and most importantly, I sincerely thank my precious and wonderful boyfriend, my lovely family and all my amazing friends for providing me inspiration and motivation through each moment of struggle during my master!

Norwegian University of Life Sciences

Ås, 12th May 2016

_____

Sigrid Aslaksen

Abstract

Embryonic stem cells have a huge potential in the field of tissue engineering, biomedical research and regenerative medicine as they possess the capacity to generate every type of cell and tissue in the body. The ability to control and manipulate embryonic stem cells to differentiate into the cell type of interest requires knowledge about the molecular principles governing early differentiation events. Several regulating pathways have been identified to have strong effects on cell fate commitment, such as the pleiotropic WNT signaling pathway and the major anabolic pathway AKT/mTOR. However, more research is needed to fully understand how the molecular mechanisms behind these two pathways and their signaling crosstalk integrate in early differentiation of embryonic stem cells.

This study demonstrates that the critical proteins, involved in these two pathways, are regulated biphasically during endodermal differentiation of human embryonic stem cells. Notably, the changes in the activity of AMPK, the major activator of catabolic processes, are clearly inversely related to the changes in the activities of mTOR and AKT throughout the differentiation process. Moreover, AMPK appeared to be highly activated towards the end of the endodermal differentiation process, concomitantly with reduced activity of AKT/mTOR, thus revealing that there is a stimulation of catabolic processes during stem cell fate commitment. Development of endoderm requires high activity of the WNT signaling pathway. Using a pharmacological inhibitor of TNKS1 and 2, this study demonstrates that GSK-3β inhibition-mediated stimulation of WNT signaling and the effects of TNKS1 and 2 on downstream components during endodermal differentiation, can be efficiently reversed. As a result, the endoderm differentiation program becomes blocked, raising the possibility that the activity of TNKS1 and 2 is crucial for a proper endodermal differentiation. Combined, this study has expanded our understanding of the molecular mechanisms underlying early differentiation steps of embryonic stem cells.

Sammendrag (Norwegian abstract)

Embryonale stamceller har vist seg å ha et stort potensial innen biomedisinsk forskning og medisinsk behandling fordi de har evnen til å differensiere til alle celletyper. For å kunne kontrollere og manipulere embryonale stamceller i den tidlige differensieringen, er kunnskap om de molekylære prinsippene som ligger bak de første trinnene viktig. Flere cellesignaliseringsveier har blitt funnet å være viktige for reguleringen av denne differensieringsprosessen, blant annet den pleiotropiske WNT signalveien og den viktige anabolske signalveien AKT/mTOR. Forståelsen av hvordan de molekylære mekanismene bak disse signalveiene er involvert i tidlig differensiering er ufullstendig og mer forskning er påkrevd.

Denne studien viser at proteinene, involvert i WNT og AKT/mTOR signalveiene, reguleres i et bifasisk mønster under utviklingen av endoderm generert fra humane embryonale stamceller. I tillegg ble det funnet at det er en motsatt sammenheng mellom aktiveringen av AMPK (viktig aktivator av katabolske prosesser) og aktiveringen av AKT/mTOR signalveien i løpet av differensieringsprosessen. Mot slutten av prosessen var AMPK kraftig aktivert samtidig som aktiviteten til AKT/mTOR signalveien var redusert. Dette tyder på at humane embryonale stamceller får økt aktivering av katabolske prosesser under differensieringsforløpet mot endoderm. Tidligere studier har vist at utviklingen av endoderm er sterkt knyttet til stimulert aktivitet av WNT signalveien. Ved å inhibere aktiviteten til TNKS1 og 2 i de humane embryonale stamcellene, ble det demonstrert at CHIR99021-mediert stimulering av WNT signalisering og effektene av TNKS1 og 2 på deres nedstrømskomponenter, effektivt kan reverseres. Dette førte dermed til en blokkert endoderm-utvikling, noe som kan tyde på at differensiering mot endoderm er avhengig av aktiviteten til TNKS1 og 2. Samlet sett har denne studien utvidet vår forståelse av de molekylære mekanismene som ligger bak tidlig differensiering av embryonale stamceller.

Table of Contents

1 Introduction

1.1 General introduction

Embryonic stem cells (ESCs) are characterized by their unique ability to both self-renew and differentiate into every cell type in our body, and offer great promise for tissue replacement therapy as they represent a renewable source of cells and tissue [1]. Over the past few decades, numerous signaling pathways have been identified to regulate the early developing embryo [2]. So far, signaling pathways activated by extracellular proteins including activin A, bone morphogenetic proteins (BMPs), fibroblast growth factors (FGFs) and Wingless-type mouse mammary tumor virus integration site proteins (WNTs) have been shown to have the strongest effects on key events during embryogenesis [3]. The WNT family of signaling proteins consists of glycoproteins that upon binding to WNT receptors induce intracellular signaling cascades, including the canonical WNT/β-catenin signaling pathway resulting in transcription of WNT target genes [4-6]. Collectively, the pleiotropic WNT pathways control multiple events during development [4-6] and it has previously been shown that up-regulation or attenuation of WNT signaling may result in different lineage-specific differentiation programs [7-9].

Recent studies have also explored the emerging role for changes in energy metabolism and activation of catabolic processes in ESC differentiation [10-13]. These cellular changes have a crucial role in exiting cells from a stem cell status and ensuring a successful differentiation to more specialized cell types with distinct energetic biosynthetic requirements [10, 13]. Notably, the major anabolic pathway AKT/mammalian target of rapamycin (AKT/mTOR) has been shown to be involved in ESC transformation, in which it negatively regulates autophagy, a process that remodels cellular components necessary for proper differentiation [10, 14]. Importantly, AKT/mTOR signaling cross talks with WNT signaling through GSK-3β, depending on the energy status of the cell [15] .

To be able to take advantage of ESCs' therapeutic potential and manipulate them to differentiate into the cell type of interest, investigation of the molecular mechanisms underlying these differentiation-determining factors is required [3]. Therefore, the main objective for this study was to investigate the mechanisms of the molecular integration

between the WNT signaling pathway and the AKT/mTOR signaling pathway in early differentiation of both human and mouse ESCs.

2 The developing embryo

Shortly after fertilization, the zygote starts to differentiate and undergoes several cell division steps to form a blastocyst. A blastocyst is made up of an outer epithelial layer of trophoblast that forms the placenta and an inner cell mass that forms a layer of cells called the epiblast (Figure 2, page 5) [16]. One of the earliest specification steps in embryogenesis is the formation and organization of the three primary germ layers: Endoderm, mesoderm and ectoderm, which together give rise to all cell types that make up future tissues and organs in the body. Formation of the three germ layers occurs during gastrulation, whereby undifferentiated epiblast cells migrate through the primitive streak to form endoderm and mesoderm (Figure 1) [8, 17, 18]. The cells that remain in the epiblast give rise to the ectoderm germ layer (Figure 1) [18]. Each of the three germ layers will produce different types of specialized cells for specific organs and tissues in the body. In general, endoderm will form the epithelial lining of the digestive and respiratory system, the liver, thyroid, pancreas, gall bladder and the thymus [19]. Mesoderm gives rise to the skeleton, skeletal muscles, smooth muscles, heart, blood cells, blood vessels, spleen, kidney, fat cells, much of the connective tissues and much of the urogenital system [19]. Ectoderm will produce the central nervous system, the lens of the eye, pigment cells, hair, the epidermis and the epithelial cells of the mammary glands [19].

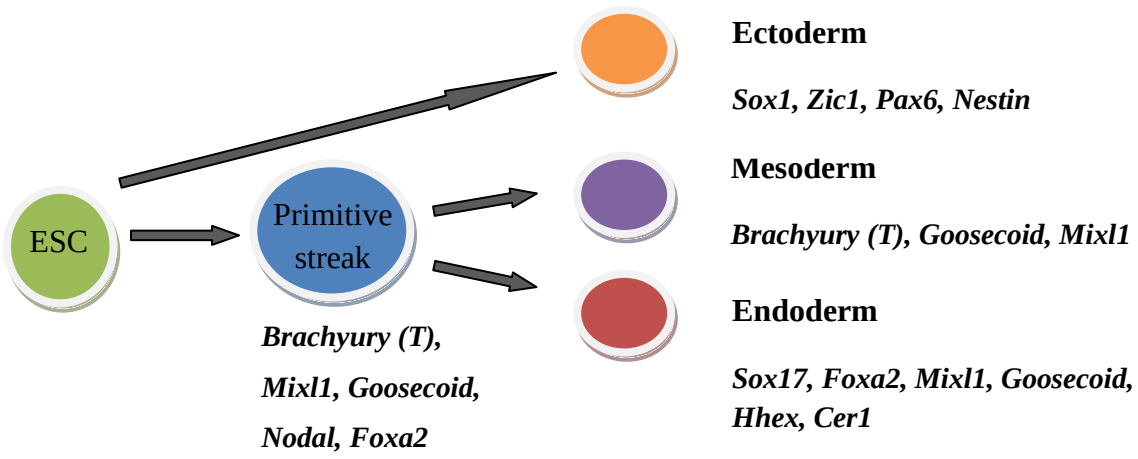

Figure 1. Formation of the three germ layers. During gastrulation, ESCs can either differentiate toward ectoderm or pass through primitive streak to generate either mesoderm or endoderm. The specific transcribed genes for primitive streak, ectoderm, mesoderm and endoderm are listed [8].

2.1 ESCs and their potential in stem cell research

To monitor the molecular and cellular mechanisms underlying the earliest events of differentiation toward the three different germ layers, researchers utilize *in vitro* ESC cultures [17]. These cells are isolated from the inner cell mass of a pre-implantation blastocyst and can subsequently proliferate to form colonies and expand into ESC cultures *in vitro* [20]. There are two essential features of ESCs that make them a robust and suitable model for stem cell research: Self-renewal, meaning that they can proliferate indefinitely without differentiating, and pluripotency, which makes them capable of differentiating towards all the three germ layers [3]. Based on these features, ESCs have a great potential in regenerative medicine and drug development, and may represent a future cure of various diseases and disabilities [17, 21]. The two most common types of ESCs used in stem cell research are mouse ESCs and human ESCs. Mouse ESCs were first isolated and cultured in 1981, whereas human ESCs were established more recently (1998) [3, 22]. Both mouse and human ESCs are powerful applications for modeling human diseases [23]. However, mouse ESCs have great potential for extensive genome manipulation in which one easily can obtain desired gene mutations to introduce or eliminate specific functions [24]. Mouse ESCs harboring relevant mutations can therefore be an important tool for studying functions of critical proteins in signaling pathways regulating key events in embryogenesis [24]. Human ESCs may have major potential in procedures using tissue engineering and regenerative medicine [1, 21, 25].

In addition to ESC research, there has also been an extensive research on the other main type of stem cells: Adult stem cells. Although these cells are often restricted to produce cell types of the organ from which they originate [21], they represent a renewable source of healthy cells that can be used in transplantation therapy [26]. Moreover, the use of adult stem cells avoids the ethical issues linked to the use of human ESC that have led governments to progress and try regulating the stem cell research. Some countries still have legislative limitations to using ESCs in research, depending on their cultural and religious viewpoints [27].

Until recently, research projects have mainly been focusing on ESCs and adult stem cells. However, in 2006, a remarkable breakthrough study [28], published by Takahashi, K. and Yamanaka, S., revealed identification of factors that could reprogram differentiated cells genetically to become embryonic-like stem cells [29]. Based on the hypothesis that unfertilized eggs and ESCs contain factors crucial for the maintenance of their pluripotency, they managed to induce pluripotency in somatic cells. These special cells were therefore called induced pluripotency stem cells (iPSCs) [28]. However, there are some issues with the use of iPSCs. First, the reprogramming process is not very efficient and only a few single cells get reprogrammed. Secondly, genomic mutations can arise from the imperfect reprogramming, causing concerns about tumorigenicity. Thus, more research is needed to be able to use them in disease modeling and to overcome iPSC safety issues [30].

2.2 Master regulators of pluripotency and self-renewal in ESCs

Previously, it has been shown that ESCs possess the potential to differentiate into multiple cell types *in vitro* [23, 31]. This capacity can remarkably be maintained even after many cell divisions, as long as they are grown under proper culture conditions that prevent further differentiation [20]. Over the last few decades, numerous transcription factors crucial for ESC pluripotency and self-renewal have been identified [32]. These factors can control the undifferentiated state by regulating their own expression in addition to the expression of other key transcription factors. Pluripotency is therefore dependent on a transcriptional network that again are regulated by epigenetic factors and specific signaling pathways [32].

There are three core transcription factors that together regulate central aspects of the transcriptional network responsible for pluripotency and self-renewal in ESCs: Nanog homeobox (NANOG), octamer-binding transcription factor 4 (OCT4) and sex-determining region Y, box 2 (SOX2) [33]. By binding to their own promoters, NANOG, OCT4 and SOX2 can positively regulate their expression [32, 34]. NANOG controls the decision point between

epiblast and primitive endoderm in the late blastocyst (Figure 2). OCT4 specifies the inner cell mass during early embryonic development and maintains the pluripotent state by inhibiting trophectoderm differentiation, which is the first forming lineage (Figure 2) [33, 34]. Similar to OCT4, SOX2 is also expressed in the inner cell mass and is required for the maintenance of the pluripotency capability of ESCs (Figure 2). Moreover, changes in SOX2 expression induce differentiation: Up-regulated expression results in neuroectodermal differentiation, whereas *SOX2* deletion induces trophectoderm differentiation [32].

Although the core transcription factors regulating pluripotency are the same in mouse ESCs and human ESCs, their gene expression is activated by different signaling pathways. This is mainly because they derive from different developmental stages, whereby mouse ESCs represent a more naïve state compared to human ESCs which are isolated at a later stage when epiblast differentiation is initiated [3]. With regard to the ease of manipulating "naïve" pluripotent stem cells, scientists try to develop methods enabling human ESCs isolation from early human embryos before they enter the epiblast stage [3].

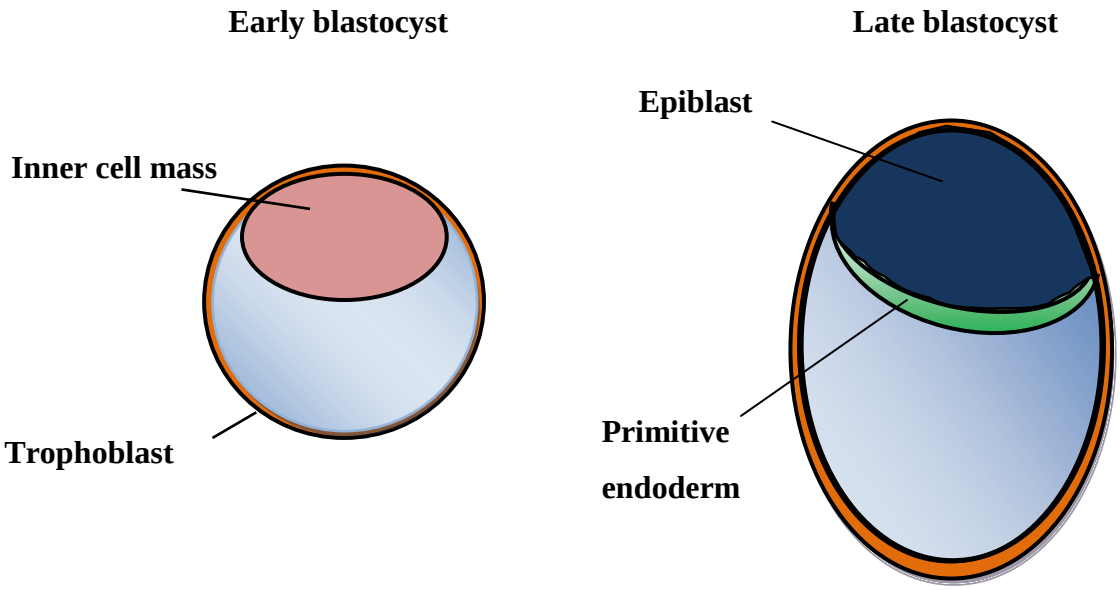

Figure 2. Overview of the roles of the key transcription factors, NANOG, OCT4 and SOX2, which cooperatively regulate pluripotency and self-renewal in ESCs. Whereas OCT4 and SOX2 specify the inner cell mass in the early blastocyst (left) and inhibits trophectoderm differentiation, NANOG controls the formation of the epiblast and primitive endoderm in the late blastocyst (right) [32].

2.3 Signaling pathways and extrinsic factors in cell fate commitment

Over the past few decades, numerous signaling pathways, activated by different extrinsic signaling molecules, have been identified to be involved in regulating the balance between maintaining pluripotency and inducing differentiation from ESCs toward lineage-committed cells [35-43]. Since mouse ESCs and human ESCs have different developmental origins, they require distinct growth factors and cytokines to activate or suppress specific intracellular signaling pathways [3].

2.3.1 LIF/JAK/STAT3 pathway

In regard to culturing mouse ESCs, the cytokine leukemia inhibitory factor (LIF) is one important extrinsic molecule, which in combination with serum or the key signaling factor bone morphogenetic protein 4 (BMP4), supports self-renewal [44]. LIF primarily inhibits mesoderm and endoderm differentiation through the Janus kinase/signal transducer and activator of transcription (JAK/STAT) signaling pathway [45]. By binding to the leukemia inhibitory factor receptor/glyco protein 130 (LIFR/gp130) receptor, LIF activates the JAK-STAT signaling pathway, resulting in gene expression of signal transducer and activator of transcription 3 (STAT3), which subsequently activates gene expression of pluripotency transcription factors, such as *Nanog* (Figure 3) [32]. Historically, mouse ESCs were co-cultured with a feeder cell layer that secreted LIF. However, previous research has demonstrated that addition of recombinant LIF to ESC cultures can sufficiently replace feeder cells [20]. In contrast, LIF/STAT3 signaling fails to maintain pluripotency and self-renewal in human ESCs, suggesting that LIF/STAT3 signaling is only required for naïve pluripotency.

Presence of LIF can also activate another important pathway, the phosphoinositide 3-kinase/AKT (PI3K/AKT) pathway, which is involved in proliferation, apoptosis and the maintenance of mouse ESC self-renewal (Figure 3). Consequently, AKT signaling will decline along with mouse ESC differentiation [46].

Mouse ESC

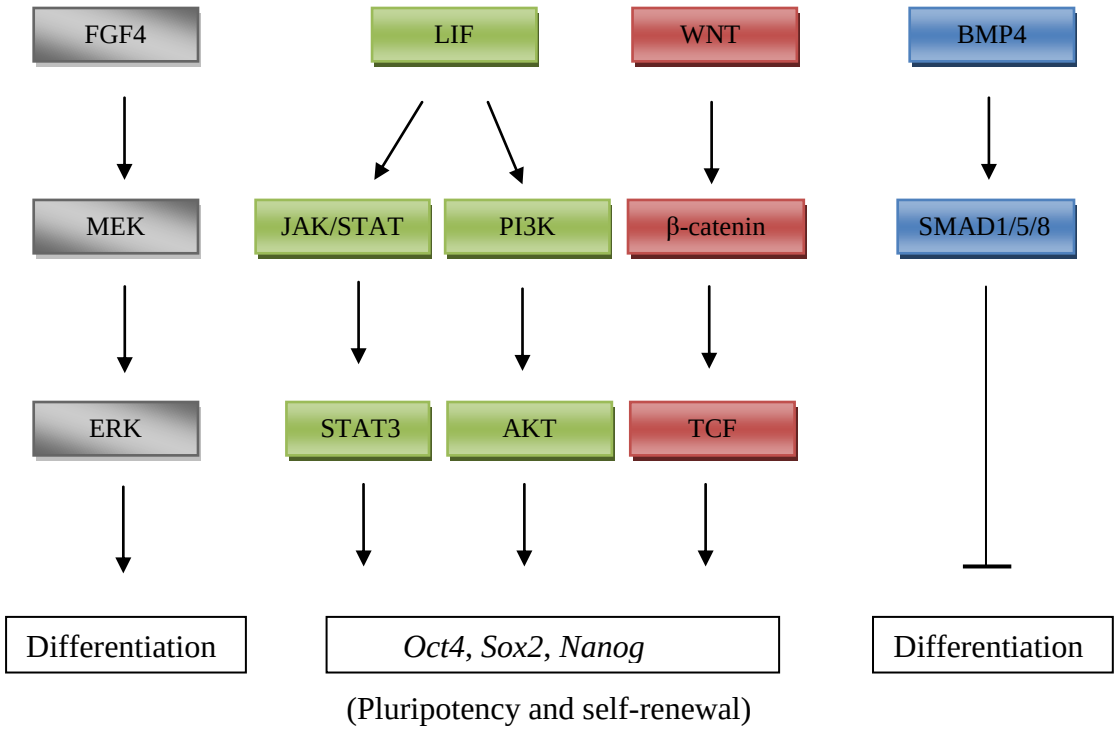

Human ESC

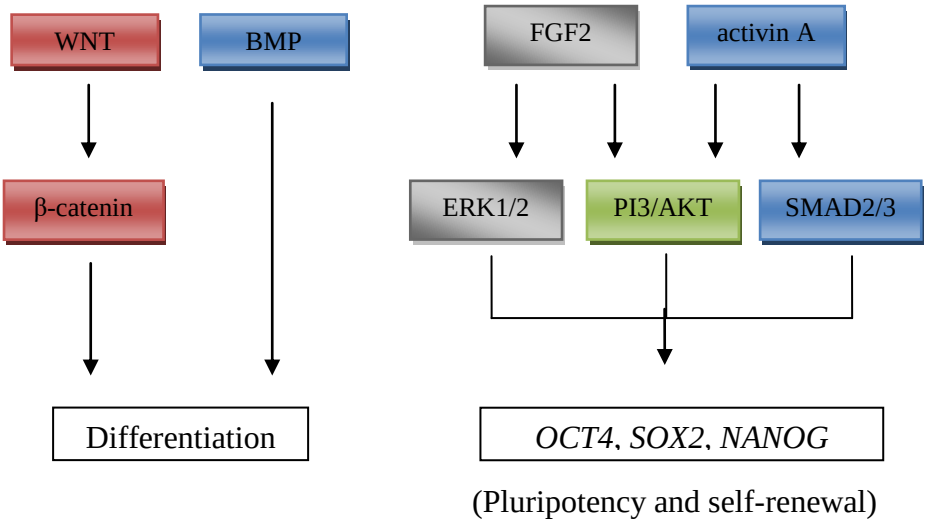

Figure 3. Simplified model of the main signaling pathways regulating self-renewal and pluripotency in mouse ESCs and human ESCs. Mouse ESC pluripotency and self-renewal depend on LIF activating the JAK/STAT and PI3K/AKT pathways, and on activation of WNT/β-catenin/TCF signaling. In contrast, FGF signaling induces differentiation through the MEK/ERK pathway, whereas BMP signaling suppresses differentiation through the activation of intracellular SMADs. Human ESC pluripotency and self-renewal is dependent on FGF2 activation of ERK1/2, PI3K/AKT and on the activation of activin signaling pathways. On the other hand, active WNT/β-catenin and BMP signaling induces differentiation [43].

2.3.2 (TGF-β) signaling

The transforming growth factor β (TGF-β) super-family consists of several distinct ligands, including TGF-β proteins, BMPs, activin A and NODAL, which bind to heterodimeric receptor complexes to initiate the SMAD signaling pathway [45, 47, 48]. Intracellular SMAD proteins can subsequently activate or repress transcriptional activity that plays an important role in pluripotency and cell fate regulation. SMAD1, SMAD5 and SMAD8 are activated by BMP ligands, whereas SMAD2 and SMAD3 are activated by activin A, NODAL and TGF-β ligands (Figure 3) [47]. These SMADs can subsequently form a complex with SMAD4 and translocate into the nucleus to regulate gene expression [45].

In mouse ESCs, the signaling factor BMP suppresses neural differentiation by inducing expression of *inhibitor of differentiation (Id)* genes through the activation of the SMAD signaling pathway (Figure 3) [45]. In human ESCs, however, BMP signaling promotes mesoderm and trophectoderm differentiation (Figure 3) [49]. Human ESC pluripotency can therefore be maintained by a NOGGIN-mediated antagonism of BMP signaling [50]. In addition, human ESC pluripotency rely on activin/NODAL/SMAD2/3 signaling (Figure 3) [45, 47]. Previous studies have demonstrated that activin/NODAL signaling can activate SMAD2/3, which subsequently initiates transcription of the pluripotent transcription factor NANOG by binding to its promoter. NANOG can then interact with SMAD2/3 to maintain expression of pluripotency genes [51] .

2.3.3 FGF/MEK/ERK pathway

Another important pluripotency-associated pathway is the FGF signaling pathway [52]. Through the mitogen-activated protein kinase kinase/extracellular signal-regulated kinase (MEK/ERK) signaling pathway, FGF4 can instruct mouse ESCs to exit from the self-renewal program and begin differentiation (Figure 3) [52]. This pathway, however, can be suppressed by small molecular inhibitors, such as PD0325901 (MEK inhibitor), in order to maintain pluripotency and self-renewal [45, 52].

FGF signaling is also important for the regulation of pluripotency in human ESCs. A recent study discovered that endogenous FGF2 signaling stimulates expression of stem cells genes

and cell survival and is maintained by exogenous FGF2 [53]. The signaling pathways activated downstream of FGF2 includes the ERK1/2 pathway, the activin/SMAD2/3 pathway and the PI3K/AKT pathway (Figure 3), which together play an important role in maintaining pluripotency [45, 53, 54].

2.3.4 Canonical WNT/β-catenin signaling pathway

Over the last few years, the canonical WNT/β-catenin signaling pathway has emerged as a critical regulator of the decision point between stem cell maintenance and differentiation, in addition to its regulation of several other developmental events including proliferation, migration, apoptosis and cell polarity [4-6, 55, 56]. However, the precise role of WNT/β-catenin signaling in ESCs is yet not fully understood as results from published studies are contradictory, showing that the WNT pathway can both promote ESC self-renewal and initiate differentiation [57]. A possible explanation for this controversial role of WNT signaling, comes from the analysis of embryonic development showing that the WNT pathway functions differently at different times during embryogenesis [40].

The different interactions that together constitute the canonical WNT signaling cascade have long been studied. One simplified model suggests that in the pathway off-state, no WNT ligand is present to induce the WNT signaling casacade resulting in a constantly degradation of cytoplasmic β-catenin by the destruction complex [56]. There are mainly four scaffold proteins that together form this complex: the axis inhibition proteins (AXIN1 and 2) [58-60], the adenomatous polyposis coli (APC) [61-63], the casein kinase 1α (CK1α) [64-66] and the glycogen synthase kinase 3β (GSK-3β) (Figure 4) [67, 68]. Initially, β-catenin interacts with the complex by binding to the scaffolding proteins AXIN and APC, which positions the N-terminal of β-catenin close to GSK-3β. CK1α then binds and phosphorylates β-catenin at serine-45 in order to prime the subsequent phosphorylations at threonine-41, serine-37 and serine-33 done by GSK-3β [69]. In addition to β-catenin phosphorylation, CK1α and GSK-3β phosphorylate AXIN and APC, increasing the interactions within the complex [69, 70]. Phosphorylated β-catenin is then recognized by the E3 ubiquitin ligase β-transducin-repeat-containing protein (β-TrCP), and the subsequent ubiquitination is recognized by the proteasome (Figure 4) [69]. β-catenin is then degraded and cannot enter the nucleus in order

to stimulate transcription of WNT target genes, such as AXIN2 [70]. Importantly, AXIN is the rate limiting factor in the formation of the destruction complex and represents therefore the key regulator in the β-catenin degradation [71]. Notably, since AXIN2 is a WNT target gene that is up-regulated upon stimulation of the WNT pathway, in addition to being an important factor of the destruction complex, it acts as a negative-feedback regulator of WNT signaling [72].

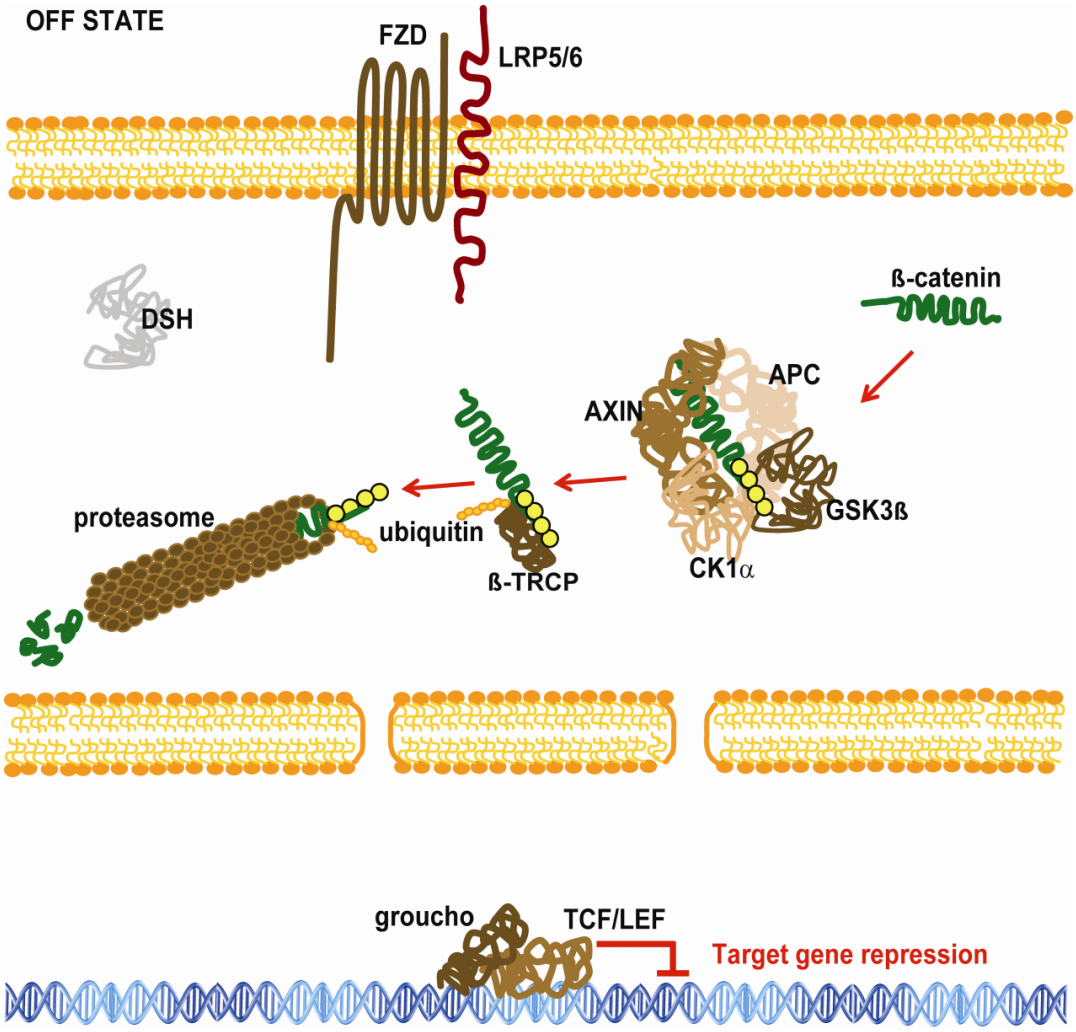

Figure 4. Canonical WNT signaling off state. In the absence of WNT ligands, cytoplasmic β-catenin interacts with the destruction complex, consisting of AXIN, APC and the two kinases CK1α and GSK-3β, and is phosporylated by CK1α and then by GSK-3β. The phosphorylations of β-catenin are recognized by β-Trcp which targets β-catenin for ubiquitination-degradation. Expression of WNT target genes is suppressed by the interaction between TCF/LEF and the transcriptional repressor groucho [56].

In the canonical WNT pathway on-state, however, WNT ligands, such as WNT1 and WNT3A [73, 74], bind the Frizzled (FZD) receptor and the co-receptor low density lipoprotein receptor-related protein 5/6 (LRP5/6) at the cell surface resulting in an activation of the WNT intracellular signaling cascade (Figure 5) [70]. The formation of the WNT-FZD-LRP signalosome complex, together with its interaction with Dishevelled (DVL), leads to recruitment and relocation of AXIN to the signalosome (Figure 5) [75-77]. AXIN can subsequently bind CK1γ and GSK-3β, which together phosphorylate LRP5/6 [70, 78-80]. As a result, AXIN cannot bind and mediate phosphorylations of β-catenin leading to β-catenin stabilization. Active β-catenin can then continuously enter the nucleus where it interacts with the transcription factors T cell factor/lymphoid enhancer factor (TCF/LEF) family of proteins to initiate transcription of WNT target genes (Figure 5) [70]. In the absence of β-catenin, TCF/LEF interacts with groucho proteins, suppressing expression of WNT target genes (Figure 4) [81].

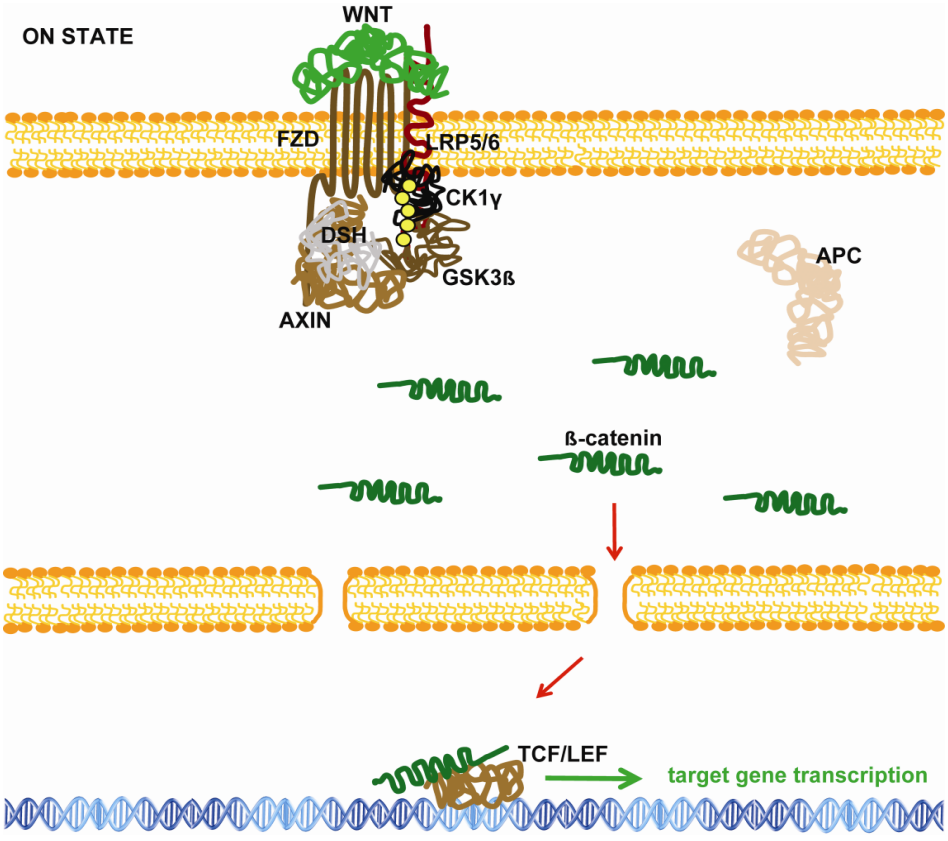

Figure 5. Canonical WNT signaling on state. In the presence of WNT ligands, the WNT-FZD-LRP signaling complex forms and binds DVL resulting in the recruitment of AXIN and LRP5/6 phosphorylation by CK1γ and GSK-3β. Together, these events result in inactivation of the destruction complex and stabilization of β-catenin. Active β-catenin can then translocate to the nucleus where it interacts with the TCF/LEF transcription factors to induce transcription of WNT target genes [56].

2.4 WNT signaling pathway regulation of ESC self-renewal

So far, three hypotheses have been proposed on the role of WNT/β-catenin signaling in maintaining pluripotency in ESCs and all of them suggest that the WNT signaling acts on the core pluripotency transcriptional network (Figure 3). The first hypothesizes that stabilized β-catenin can inactivate the TCF3 mediated repression of the core pluripotency transcriptional network involving NANOG, OCT4 and SOX2 [82]. Previous studies have reported that TCF3 binds to the same promoters as NANOG, OCT4 and SOX2, thereby repressing their positively regulation of their own genes [40, 83-85]. Thus, TCF3 is a component in the regulatory network controlling pluripotency and self-renewal. Upon activation of WNT signaling, stabilized β-catenin may relieve this repression through its interaction with TCF3 [57, 86]. The second hypothesis claims that β-catenin/TCF mediated transcription has an important role in maintaining pluripotency in which the TCF1 and the LEF1act as important mediators of WNT stimulation of pluripotency and self-renewal in ESCs [40, 85]. The last hypothesis claims that pluripotency is promoted through a direct interaction between β-catenin and OCT4 resulting in an up-regulation of *NANOG* expression [87]. However the precise role of this interaction during ESC self-renewal remains unclear [57].

Previous research has shown that WNT signaling seems to play opposite roles in the regulation of self-renewal and pluripotency in mouse ESCs and human ESCs [88-90]. This is possibly due, at least in part, to their different developmental origins. With respect to pluripotent mouse ESCs, active WNT signaling promotes expression of OCT4, NANOG and SOX2 (Figure 3) [45], inhibits neuroectodermal differentiation and specifies the mesendodermal lineage [40]. One common extrinsic factor used to promote pluripotency in mouse ESCs, also used in this study, is the small molecule named CHIR99021, which inhibits GSK-3β resulting in active WNT signaling [90]. In contrast, active WNT signaling - and stabilized β-catenin in human ESCs have been shown to induce rapid differentiation toward primitive streak, endoderm and mesoderm (Figure 3) [37, 38]. Moreover, WNT signaling in self-renewal human ESCs seems to be repressed by the key pluripotency transcriptional factor OCT4 [88]. However, the precise role of WNT/β-catenin signaling in human ESCs is still under debate and requires further research [40, 88].

2.5 Tankyrases 1 and 2 - promising targets for regulating WNT/β-catenin signaling

Aberrant WNT/β-catenin signaling activity due to mutational events in the WNT pathway may lead to various diseases and cancers [5, 6, 70]. These mutational events involve inactivating mutations in APC or AXIN and activating mutations of β-catenin, and can lead to accumulation of nuclear β-catenin that promotes tumor initiation and growth [56]. Consequently, there has been extensive research on how to control and inhibit the pathway at multiple levels [56]. Recent studies have revealed identification of some small-molecule inhibitors of the pathway. So far, tankyrase (TNKS) has been identified to be one of the most promising targets for drugs being developed, due to its ability to promote degradation of AXIN (Figure 6A) [56]. As mentioned earlier, AXIN is the rate limiting structural protein in the destruction complex and is therefore also a key regulator of β-catenin degradation [56, 91]. Thus, inhibition of TNKS can attenuate WNT signaling through an increased stability of AXIN and the destruction complex, which promotes degradation of β-catenin (Figure 6B) [91]. Moreover, this increased stability of destruction complexes has been shown to decrease WNT signaling in cells containing wild-type APC and in colorectal cancer (CRC) cells containing truncated APC (Figure 6B) [92-94]

TNKS belongs to the Diphtheria toxin-like adenosine diphosphate (ADP)-ribosyltransferase (ARTD) enzyme superfamily [95] and can control a variety of cellular functions, such as WNT/β-catenin signaling, maintenance of the telomere length, translocation of glucose transporter type 4 (GLUT4)-containing vesicles important for insulin-stimulated glucose uptake and cell cycle progression [91, 96-98]. The two similar isoforms, TNKS1 and 2 have multiple domains: i) The catalytic ADP-ribosyltransferase (ART) domain also known as the poly (ADP-ribose) polymerase (PARP) domain, responsible for poly (ADP-ribose)sylate (PARsylate) target proteins after cleaving nicotinamide adenine dinucleotide (NAD^+) into nicotidamide and ADP-ribose. ii) The sterile alpha motif (SAM) domain located downstream of the PARP domain, which mediates protein-protein interactions. iii) Five ankyrin repeat clusters that interact with target proteins [91]. PARsylated proteins are recognized and subsequently poly-ubiquitinated by the E3 ubiquitin ligase and finally degraded by the proteasome [91]. In addition, TNKS may also PARsylate itself (autoPARsylation) controlling

its own stability and activity [91, 92]. In the context of WNT signaling, TNKS1/2 can bind and PARsylate AXIN, which is then targeted for proteasomal degradation by the ubiquitin E3 ligase ring finger protein (RNF146) leading to active WNT signaling (Figure 6A) [91].

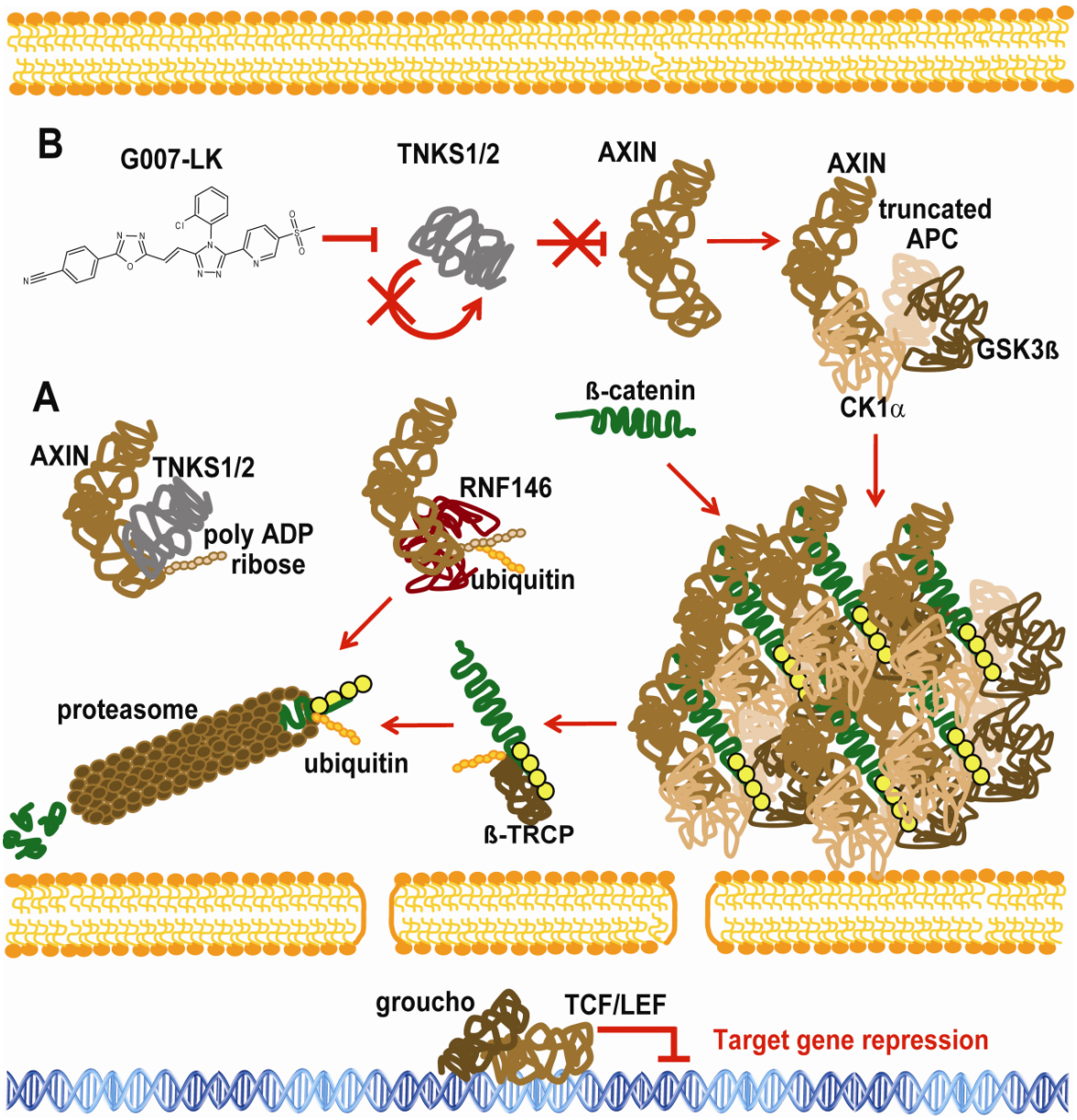

Figure 6. TNKS' role in the WNT signaling pathway. (A) TNKS acts as an important component in the WNT signaling pathway in which it interacts with AXIN, and tags it with ADP-riboses (PARsylation). The poly ADP-ribose chain is subsequently recognized by RNF146 that poly-ubiquitinizes AXIN, which is further degraded in the proteasome. (B) The TNKS inhibitor G007-LK inhibits the PARP domain of TNKS leading to AXIN stabilization and accumulation of the destruction complex. Phosphorylation of β-catenin may then be enhanced by the complex preventing β-catenin from entering the nucleus and induce WNT target gene expression [56].

2.5.1 Inhibition of TNKS

Present TNKS inhibitors are engineered to bind to the catalytic ART/PARP domain and can be divided into two groups depending on their specific binding site: i) XAV939 is an example of a compound that binds the nicotinamide pocket [92] where the hydrolysis of the NAD^+ occurs [91]. ii) JW55 and G007-LK are compounds that bind to the adjacent adenosine binding pocket where the transfer of an ADP-ribose to a target protein occurs [91]. The TNKS1/2 inhibitor used in this study, G007-LK, has been shown to be highly selective and stabile against enzymatic degradation [91, 99, 100]. Previous research has demonstrated that cancer cell growth, induced by WNT signaling, treated with G007-LK show stabilization of AXIN and reduction of canonical WNT signaling (Figure 6B) in both *in vitro* and *in vivo* [99, 100].

2.6 The WNT signaling pathway's regulatory role in ESC fate commitment

When stimulating the process of ESC differentiation, the WNT pathway can either be up-regulated or downregulated resulting in an initiation of multiple differentiation programs [101]. With respect to mouse ESCs, up-regulation of WNT signaling, using WNT ligands including WNT3A, may induce primitive streak formation and mesendodermal differentiation [8], whereas inhibition of WNT signaling, appears to promote neuroectodermal differentiation [40, 102]. Similar observations have also been reported in human ESCs; altered levels of WNT signaling in human ESCs drive them toward distinct lineage-specific differentiation. Human ESCs with low WNT signaling will have an enhanced ability to differentiate towards a neuroectodermal lineage, while human ESCs having high WNT activity are more primitive streak like and can differentiate into endodermal and mesodermal cells [7, 9]. This can partly be explained by the WNT pathway's positiv regulatory role in SOX17 expression, which facilitates the differentiation toward endoderm [103]. Previous studies have therefore utilized

small-molecules that stimulate WNT signaling, such as GSK-3β inhibitors, when aiming to prime human ESCs for endodermal differentiation [9, 104].

2.7 Crosstalk between the WNT signaling pathway and the AKT/mTOR signaling pathway and the involvement of AMPK

Metabolism is the sum of all chemical reactions within living cells and organisms, and can be divided into two categories: Catabolism, which involves breakdown of molecules to release energy used for driving all cellular processes, and anabolism, which involves synthesis of all cellular compounds such as proteins, nucleic acids and lipids [105]. Protein and lipid metabolism is regulated by various factors including adenosine monophosphate-activated protein kinase (AMPK) [106]. This is a well-conserved energy sensor capable of switching off anabolic pathways including fatty acid and protein synthesis, and switching on catabolic pathways including fatty acid oxidation and glycolysis [107]. AMPK is composed of a catalytic α subunit and, β and γ regulatory subunits [108]. It is activated by various types of metabolic stress that leads to changes in adenosine monophosphate/adenosine triphosphate (AMP/ATP) ratios, such as low nutrient supply or prolonged exercise [109]. The main activation process happens when the liver kinase B1 (LKB1) phosphorylates threonine-172 (Thr172) in the activating loop of the catalytic α-subunit of AMPK upon increased levels of AMP/ADP (Figure 7) [109]. Once activated, AMPK phosphorylates a variety of substrates to stimulate catabolic activities that maintain intracellular ATP levels, such as autophagy [108, 110]. A previous study has demonstrated that AMP is critical in the activation process in which it drives AMPK to interact with the scaffolding protein AXIN [111]. AXIN can then bind to LKB1 to form the AXIN/LKB1-AMPK complex [111], which may facilitate the phosphorylation of AMPK by bringing it close to LKB1 (Figure 7) [107].

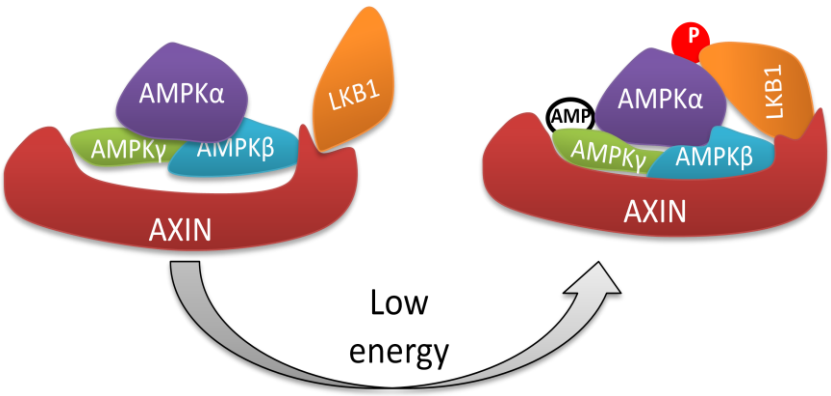

Figure 7. Simplified model of the AMPK activation process. Under a low cellular energy state, AMP binds to the AMPKγ subunit driving AMPK to bind AXIN, which subsequently binds LKB1. AMPK is then activated by a LKB1 phosphorylation of the AMPKα subunit [107].

Under nutrient-rich conditions, however, growth factors stimulate anabolic processes by activating the PI3K/AKT pathway [108]. The activating process of AKT involves phosphorylation at its serine-473 (Ser473) and threonine-308 (Thr308) residues [112]. Activated AKT can then go on to inhibit the tuberous sclerosis complex (TSC) by phosphorylation which in turn leads to an activation of the mTOR pathway (Figure 8) [110]. In addition, phosphorylated AKT can also phosphorylate serine-9 (Ser9) in the N-terminus of GSK-3β, thereby inhibiting its catalytic activity including its phosphorylation of primed substrates involved in glycogen synthesis (Figure 8) [108]. Furthermore, activation of AKT has also previously been shown to rely on the activity of mTOR in which mTOR can phosphorylate AKT at Ser473, thereby enhancing AKT/mTOR signaling (Figure 8) [113]. Cooperatively, these events stimulate protein and lipid synthesis and cell growth (Figure 8) [108].

The TSC complex, downstream from AKT, consists of the TSC1 and TSC2 proteins encoded by the tumor-suppressor genes *TSC1* and *TSC2* [15]. TSC2 is the catalytic subunit of the complex having guanosine triphosphate (GTP)ase-activating protein (GAP) activity toward Ras homolog enriched in brain (RHEB) (a GTPase protein of the Ras superfamily) converting it from its GTP-bound active state to its guanosine diphosphate (GDP)-bound inactive state [15, 114]. However, active RHEB may bind and activate the mTOR complex 1 (mTORC1), which subsequently phosphorylates two critical protein translation regulators, p70 ribosomal protein S6 kinase (p70S6K) and eukaryotic initiation factor 4E binding protein 1 (4EBP1)

(Figure 8) [15, 114, 115]. In this study, the focus will be on the phosphorylation of p70S6K at threonine-389 (Thr389) and the following phosphorylation of ribosomal protein S6 (RPS6) at serine-240/244 (Ser240/244). Together, these phosphorylations have been demonstrated to correlate with an increased translation of messenger ribonucleic acid (mRNA) encoding proteins and cell growth (Figure 8) [115-117].

TSC1 and TSC2 are not only phosphorylated by AKT, but by several other kinases linking multiple signaling pathways to the regulation of mTOR signaling and cell growth [15]. A previous study demonstrated that one of these pathways is the WNT signaling pathway, which can regulate the TSC-mTOR pathway via GSK-3β, independently of β-catenin induced transcription [15]. GSK-3β can phosphorylate and activate TSC2 resulting in an active TSC complex and inhibition of mTOR signaling (Figure 8). This can be blocked by stimulating WNT signaling (Figure 8) [15]. Further, the activating GSK-3β phosphorylation of TSC2 is dependent on a primed phosphorylation by AMPK (Figure 8) [15]. As mentioned earlier, AMPK has been identified to be a critical sensor of the cellular energy status [15, 108]. Collectively, these results suggest that AMPK has a critical role in the coordination of cell growth and cellular levels.

Regulation of the TSC/mTOR pathway by WNT signaling may not only be coordinated by the action of GSK-3β; several other WNT signaling components including DVL, AXIN, APC have been identified to be important for this regulation [15]. These findings can be related to a previous report, whereby TSC2 was shown to interact with GSK-3, AXIN and DVL by co-immunoprecipitation [118]. Thus, AXIN may work as a scaffold protein bringing TSC2 close together with GSK-3 and AMPK, which may facilitate the phosphorylation of TSC2. Therefore, AXIN plays the same role in the activation of the TSC complex as it does in the phosphorylation of AMPK [107, 111].

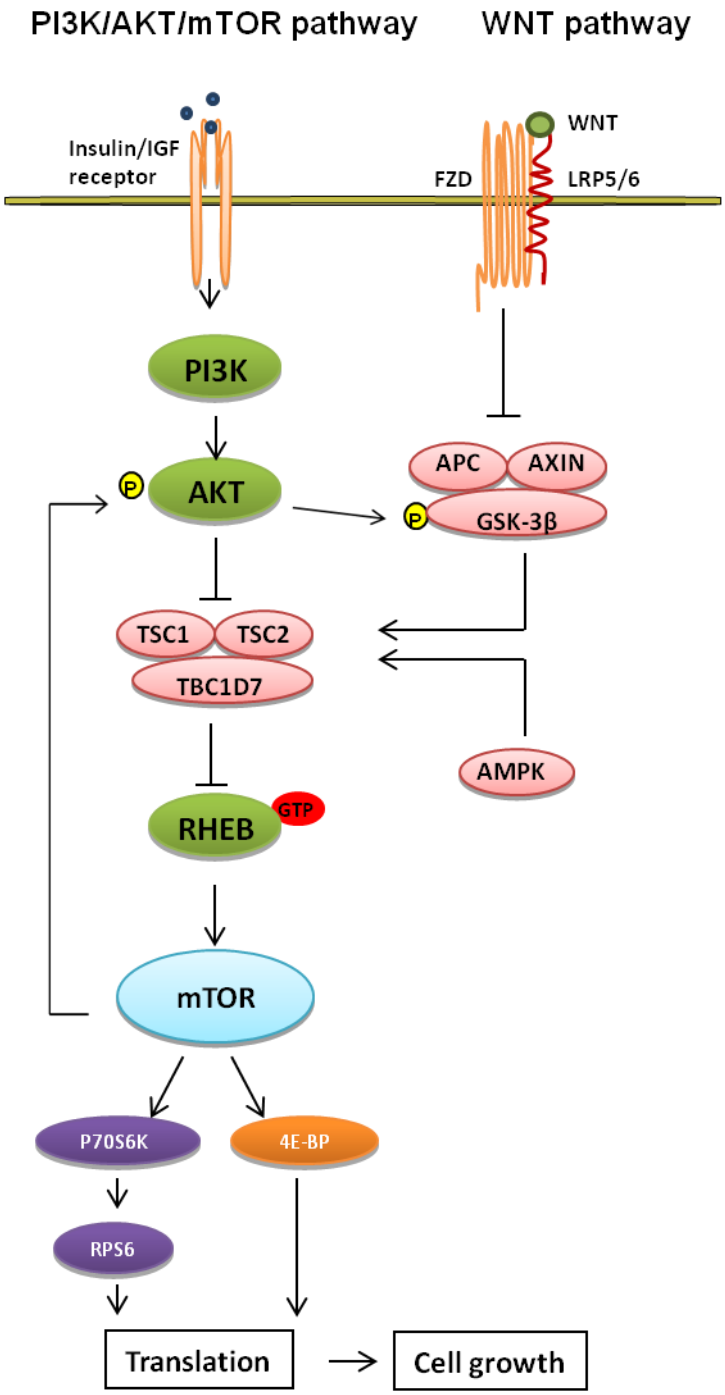

Figure 8. Simplified model of the signaling crosstalk between the PI3K/AKT/mTOR pathway and the WNT pathway. Growth factors such as insulin stimulate PI3K to phosphorylate AKT, which subsequently can inhibit the TSC complex. GTP-bound RHEB can further activate p70S6K and 4E-BP by activating mTORC1. Phosphorylated p70S6K can further activate RPS6, which leads to an increased mRNA translation and cell growth. In contrast, inhibition of the mTOR pathway is induced by activating the TSC complex. This activation involves a GSK-3β phosphorylation of TSC2, which requires an AMPK primed TSC2 phosphorylation. The TSC complex can then inhibit RHEB suppressing mTOR signaling [110].

2.8 Metabolic changes linked to pluripotency and differentiation of ESCs

In the past few years, several studies have revealed interesting results showing that energy metabolism, involving the metabolic pathways, has a key role in the decision point between pluripotency maintenance and differentiation of ESCs [10-12]. Due to the hypoxic environment inside the blastocyst from which they were retrieved, ESCs are restricted to drive anaerobic glycolysis even when they are cultured in atmospheric oxygen [10, 12]. Upon differentiation, this metabolic state switches: The anaerobic glycolysis gets downregulated and the immature mitochondria of pluripotent ESCs develops, enabling the cells to oxidize most of the pyruvate, produced by glycolysis, in the mitochondria via oxidative phosphorylation (OXPHOS) [10, 12]. These findings therefore demonstrate that pluripotency and self-renewal of ESCs rely upon limited mitochondrial respiration. Furthermore, the glycolysis-derived acetyl coenzyme A (acetyl-CoA) has also been identified to play a role in the balance between pluripotency and differentiation in which it promotes histone acetylation important for pluripotent ESCs [119, 120]. Combined, these metabolic changes have been identified to be relevant for modulating chromatin plasticity and regulating histone modifications during cellular differentiation [12, 119, 120].

Shifts in energy metabolism are regulated by several transcriptional factors including v-Myc avian myelocytomatosis viral oncogene homolog (c-MYC), which is involved in inhibiting the conversion of pyruvate to acetyl-CoA [121]. Interestingly, the WNT target gene AXIN2, important for the formation of the β-catenin destruction complex, has been identified to repress expression of the WNT target gene *c-MYC*. When constitutively localized to the nucleus, AXIN2 changes the chromatin structure of the *c-MYC* promoter [122]. Thus, AXIN2 may play an important regulatory role in the metabolic changes that takes place in the first steps in ESC exit from the pluripotent state.

2.9 Aims of the study

The primary objective of this study was, in the frame of early differentiation events of ESCs, to investigate the implications i) of the WNT signaling pathway, and its molecular components such as TNKS and AXIN on differentiation, ii) implications of the major anabolic signaling pathways such as AKT/mTOR signaling on differentiation and iii) the functional interlink between the two pathways. The secondary objective was to investigate how the early differentiation, from a pluripotent state to the formation of neuroectoderm or through a primitive streak intermediate into endoderm, is affected by pharmacological TNKS inhibition. TNKS inhibition can in addition to antagonizing WNT signaling also attenuate the AKT pathway in a subtype of cancer cell lines [123]. The last aim was to assess whether stimulation of AKT/mTOR signaling throughout the differentiation process, by an AKT activator, would delay or block the formation of endoderm.

3 Materials and Methods

3.1 Cell lines and culture conditions

3.1.1 Mouse ESC culture

Two different cell lines derived from the mouse line C57BL/B6 were used: *Axin1*$^{fl/fl}$, *Axin2*$^{fl/fl}$ (wild-type) and *Axin1* $^{\Delta/\Delta}$, *Axin2* $^{\Delta/\Delta}$ (*Axin* double knockout, DKO). Generation of mouse ESCs comprising *Axin* DKO was performed by Professor Trevor Dale and his research group at Cardiff University [124]. First, a homozygous mice bearing *LoxP* - flanked *Axin1* and *Axin2* alleles was generated following a previously published method [125]. Mouse ESCs derived from *Axin1*$^{fl/fl}$ and *Axin2*$^{fl/fl}$ mice were next transfected with a plasmid expressing cre recombinase and clones in which exon2 was deleted in both *Axin1* and *Axin2* were identified.

Mouse ESCs, wild-type and *Axin1/2* mutant, were cultured on gelatin (0.1%) coated (Sigma Aldrich) culture plates in 2i culture medium [Dulbecco's Modified Eagle Medium/Nutrient Mixture F-12 (DMEM/F12) + GlutaMax (Life Technologies) medium containing 10% fetal bovine serum (FBS) ES qualified (Life Technologies), 1% penicillin-streptomycin (Sigma Aldrich), 0.5 µM of PD0325901 (Selleck Chemicals), 3 µM of CHIR99021 (Selleck Chemicals), 0.1 mM of β-mercaptoethanol (Life Technologies) and 10^6 U/l of LIF (Life Technologies)]. The cells were cultured at 37°C and 5% CO_2. The medium was changed every day and cells were split 1/3 using trypsin-ethylenediaminetetraacetic acid (EDTA) (Sigma Aldrich) every two to three days.

3.1.2 Human ESC culture

The human ESC line H1 (purchased from WiCell) was cultured under feeder free conditions using growth factor reduced Matrigel coated (Sigma Aldrich) 6-well plates (Nunc) in Essential 8 medium (Life Technologies) at 37°C and 5% CO_2. The cells were split 1/6 when they reached 80-85% confluency using 0.5 mM EDTA (Life Technologies) usually once or twice a week.

Growth and passage of the H1 cells were performed by my group's collaborating stem cell research team headed by Dr. Gareth Sullivan at the Institute of Basic Medical Science at Oslo University Hospital, Rikshospitalet.

3.2 Characterization of mouse ESC

3.2.1 Alkaline phosphatase staining

Alkaline phosphatase staining is a technique used to test stem cell pluripotency. Undifferentiated pluripotent ESCs can be characterized by high expression levels of alkaline phosphatase [126], which can be detected by alkaline phosphatase staining.

After fixing the ESCs with a premade fix solution from the Alkaline Phosphatase Staining Kit II (Stemgent), cells were stained using the Alkaline Phosphatase Staining Kit II according to the manufacturer's instructions. To perform a percentage score of alkaline phosphatase positive cells a Zeiss Axiovert 200M inverted microscope (Stanwood, Washington, USA) was used.

3.2.2 Immunofluorescence

Mouse ESCs were seeded onto 12-well plates (Nunc) coated with 0.1% gelatin in 2i medium and allowed to adhere for 24 hours at 37°C and 5% CO_2. The cells were washed with Dulbecco's Phosphate-buffered saline (PBS) (Life Technologies), fixed with ice cold methanol (VWR) for 10 min and then washed with PBS twice. Next, the cells were washed with PBS containing 0.1% Tween 20 (Sigma Aldrich) (PBS-T) and then incubated with 10% of normal goat serum (NGS) (Life Technologies) in 0.1% PBS-T for 3-4 hours at room temperature. After washing twice with PBS-T, the cells were incubated with the primary antibodies including anti-OCT4 (rabbit IgG, 1:100, Stemgent), anti-NANOG (rabbit IgG, 1:100, Stemgent) and anti-SOX2 (rabbit IgG, 1:100, Stemgent) overnight at 4°C. All primary antibodies were made up in 1% NGS in 0.1% PBS-T. Following primary incubations, the

cells were washed three times and incubated with secondary antibodies including anti-rabbit IgG Alexafluor 488 donkey antibody (1: 400, Life Technologies), anti-rabbit IgG Alexafluor 594 donkey antibody (1: 400, Life Technologies) for 1 hour at room temperature. The secondary antibodies were diluted in PBS. The cells were then washed three times with PBS-T and four times with PBS before being mounted using Fluoroshield with 4', 6-diamidino-2-phenylindole (DAPI) (Sigma Aldrich) and glass coverslips (VWR). The cells were imaged using a Zeiss Axiovert 200M inverted microscope (Stanwood, Washington, USA) and AxioVision Software (Carl Zeiss).

3.3 Culture conditions for ESC differentiation

3.3.1 Differentiation of mouse ESCs

Directed induction of primitive streak by WNT3A

For differentiation of the wild-type mouse ESCs into primitive streak, they were dissociated using 20 µg/ml EDTA in PBS. To find the optimal cell density for this primitive streak differentiation experiment, the cells were seeded at 0.75 x 10^4/cm^2, 1.2 x 10^4/cm^2, 1.5 x 10^4/cm^2, 1.7 x 10^4/cm^2 and 2.0 x 10^4/cm^2 onto 6-well plates coated with laminin (1µg/cm^2) (Sigma Aldrich) 10-15 minutes prior to use. The cells were cultured in 2i medium for 24 hours at 37°C and 5**%** CO_2 before treatment to allow cell adhesion to the culture plates. Next, the cells were washed with PBS before treated with differentiation medium. Three different types of cell mediums were tested: Knockout Dulbecco's Modified Eagle Medium (DMEM), Iscove's Modified Dulbecco's Medium (IMDM) and Roswell Park Memorial Institute (RPMI) Medium 1640 with GlutaMAX (all from Life Technologies). All three mediums contained 10 µg/ml of insulin, 5 µg/ml of apo-transferrin, 10 µM of 2-mercaptoethanol, 10 µM of ethanolamine, 10 µM of sodium selenite (all from Sigma Aldrich) and 0.5 mg/ml of BSA (Europa Bioproducts). In addition, 50 ng/ml of recombinant mouse WNT3A (R&D Systems Europe LTD.) was supplemented. The three different cell treatments lasted for 3 days and the mediums were changed every day.

To induce primitive streak using a ESF basal medium (Cell Science & Technology Institute, Sendai, Japan) containing 10 µg/ml of insulin, 5 µg/ml of apo-transferrin, 10 µM of 2-mercaptoethanol, 10 µM of ethanolamine, 20 nM of sodium selenite, 0.5 mg/ml of BSA and 50 ng/ml of recombinant mouse WNT3A, the wild-type ESCs were seeded onto laminin (1 µg/cm^2) coated culture plates at 0.75-2.0 x 10^4 cells/cm^2. The culture plates were coated with laminin 2 hours prior to use to enhance its effect.

Induction of differentiation by removal of LIF and CHIR99021

The wild-type mouse ESCs were dissociated using trypsin-EDTA and seeded onto 6-well plates coated with 0.1% gelatin at 1.5 x 10^4 cells/cm^2 (for the 24-hour treatment) and 3 x 10^4 cells/cm^2 (for the 48-hour treatment) in 2i medium for 24 hours at 37°C and 5% CO_2 to allow the cells to adhere. Two different cell densities were used to make sure that the 24-hour plate had approximately the same confluence as the 48-hour plate when the cells were harvested for quantitative real-time reverse transcription polymerase chain reaction (qRT-PCR). Before initiating the differentiation treatment, the cells were washed with PBS. Three different treatments were used: 2i medium without CHIR99021 or LIF or both. The culture medium was renewed every day. Untreated cells, cultured in 2i medium (with both CHIR99021 and LIF), were used as a control.

3.3.2 Differentiation of human ESCs

Differentiation of the human ESCs into definitive endoderm through primitive streak was performed by following the protocol published by our collaborator Gareth Sullivan and his research group [9]. First, the cells were seeded at a 1:3-1:4 split ratio onto Matrigel-coated 6-well plates in Essential 8 medium for 24 hours at 37°C and 5% CO_2 to allow the cells to adhere. Next, they were washed with PBS before initiating the differentiation process: 24 hours with RPMI Medium 1640 with GlutaMAX containing B-27 supplement with insulin (RPMI-B27) (Life Technologies) supplemented with 3 µM of CHIR99021 (Stemgent), followed by a 24-hour treatment with RPMI-B27 alone. During the 48-hour time course, the

cells were harvested for qRT-PCR and Western blot analysis at six different time points: 0, 4, 8, 12, 24 and 48 hours.

Treatment with G007-LK (TNKS inhibitor)

The human ESCs were seeded at a 1:3-1:4 split ratio onto Matrigel-coated 6-well plates in Essential 8 medium for 24 hours at 37°C and 5% CO_2 to allow cells to adhere before the G007-LK (ChemRoyal) treatment. Next, the cells were cultured in RPMI-B27 containing 3 µM of CHIR99021 along with 1µM of G007-LK [dissolved in dimethyl sulfoxide (DMSO) (Sigma Aldrich)] or 0.11% DMSO (used as a control) for 24 hours and then cultured in RPMI-B27 alone for another 24 hours. During the 48-hour time course, the cells were harvested for qRT-PCR and Western blot analysis at six different time points: 0, 4, 8, 12, 24 and 48 hours. For the Western blot analysis, two different samples at the 48-hour time point were made: One sample of cells treated with 1 µM of G007-LK for 24 hours during the differentiation process and another sample of cells treated with 1 µM of G007-LK for 48 hours during the differentiation process.

Treatment with SC79 (AKT activator)

The human ESCs were seeded at a 1:3-1:4 split ratio onto Matrigel-coated 6-well plate in Essential 8 medium for 24 hours at 37°C and 5% CO_2 to allow cells to adhere before the SC79 (R&D Systems) treatment. Next, the cells were cultured in RPMI-B27 containing 3 µM of CHIR99021 along with 2 µM or 5 µM or 10 µM or 15 µM of SC79 or 0.015% DMSO (used as a control) for 24 hours. The cells were harvested for Western blot analysis 0 and 24 hours after the start of the differentiation.

3.4 RNA isolation and qRT-PCR

Total RNA was extracted using the column-based GenElute™ Mammalian Total RNA Miniprep Kit (Sigma Aldrich) according to the manufacturer's instructions. RNA was quantified using a NanoDrop 2000c (Thermo Fischer Scientific) and 500 ng of total RNA was used for synthesizing complementary deoxyribonucleic acid (cDNA) using the High Capacity Reverse Transcription kit and a thermal cycler (both from Life Technologies). The thermal cycling conditions were as follows: 10 minutes at 25^0C, 120 minutes at 37^0C and 5 minutes at 85^0C. The synthesized cDNA was then used for qRT-PCR using a TaqMan ViiA7 Real Time PCR System with TaqMan Gene Expression Mastermix (both from Life Technologies) according to the supplier's instructions. All qRT-PCR reactions were performed in 96-well plates (Nunc) and the reaction conditions were: 30 seconds at 95^0C for polymerase activation and initial denaturation of the cDNA (initialization step), followed by 40 cycles of 10 seconds at 95^0C for further denaturation of the cDNA, followed by 20 seconds at 60^0C for annealing the primers to the target region of the single stranded cDNA and 30 seconds at 72^0C for facilitating the synthesis of a new complementary strand to the template.

Each cDNA sample was run in triplicate and the readings were analyzed by the comparative quantification method ($\Delta\Delta$ C_t) using Microsoft Excel. *β-actin* (*ACTB*), for human ESCs, and *glyceraldehyde-3-phosphate dehydrogenase* (*GAPDH*), for mouse ESCs, were used as endogenous controls (reference genes) to normalize the amount of cDNA in each sample in order to ensure comparability of the measured expression levels of mRNA in the individual samples.

The C_t (threshold cycle) value is the cycle number at which the fluorescent signal is significantly higher than the baseline (background) signal [127].

$\Delta\Delta\ C_t = (C_{t\ target}{}^{S} - C_{t\ reference}{}^{S}) - (C_{t\ target}{}^{C} - C_{t\ reference}{}^{C})$ *

* $C_{t\ target}{}^{S}$: The C_t value of the target gene in the treated sample; $C_{t\ reference}{}^{S}$: The C_t value of the reference gene in the treated sample; $C_{t\ target}{}^{C}$: The C_t value of the target gene in the untreated (control) sample; $C_{t\ reference}{}^{C}$: The C_t value of the of the reference gene in the untreated (control) sample.

To assess whether there were significantly differences between the qRT-PCR results for the cells treated with 1 µM of G007-LK and the qRT-PCR results for the untreated control cells, the one-tailed Students *t*-test was performed using Sigma Plot 13.0.

The probes used for the mouse ESC qRT-PCR analyses were as follows: *Nanog, Oct4, Sox2, Goosecoid (Gsc), Foxa2, Nodal, T, Mixl1, Sox1* and *Zic1*. The probes used for the human ESC qRT-PCR analyses were as follows: *CER1, FOXA2, GSC, HHEX, MIXL1, NODAL, SOX17, T, ACTB, PAX6* and *NESTIN*.

All the probes were ordered from Life Technologies and their gene expression assay ID numbers were as follows:

Oct4	Mouse	Mm03053917_g1	***GAPDH***	Human	Hs02758991_g1
Sox2	Mouse	Mm03053810_s1	***CER1***	Human	Hs001933796_m1
Nanog	Mouse	Mm02019550_s1	***FOXA2***	Human	Hs00232764_m1
Sox1	Mouse	Mm00486299_s1	***GSC***	Human	Hs00906630_m1
Zic1	Mouse	Mm00656094_m1	***HHEX***	Human	Hs00242160_m1
Gsc	Mouse	Mm00650681_g1	***MIXL1***	Human	Hs00430824_g1
Foxa2	Mouse	Mm01976556_s1	***NODAL***	Human	Hs00415443_m1
Nodal	Mouse	Mm00443040_m1	***SOX17***	Human	Hs00751752_s1
T	Mouse	Mm00436877_m1	***T***	Human	Hs00610080_m1
Mixl1	Mouse	Mm00489085_m1	***PAX6***	Human	Hs00240871_m1
			NESTIN	Human	Hs00240871_m1
			ACTB	Human	N/A

3.5 Western blot analysis

For protein analyses, the human ESCs were lysed in NP40 lysis buffer (Life Technologies) containing protease inhibitors (Roche Applied Science) (1 tablet/10 ml NP40 lysis buffer, 100-200 µl lysis buffer/5 x 10^5 cells). The cells were collected using cell scrapers (Starstedt) and the lysate was transferred to 1.5 ml Eppendorf tubes, followed by 15 minutes of centrifugation at 8 x g at 4°C. The Supernatant was transferred to a new tube and protein concentration was measured using the Bradford Assay (Bio-Rad), whereby the absorbance at 562 nm was measured using FLUOstart Omega microplate reader (Allmengruen, Ortenberg, Germany). The protein samples were then mixed with sodium dodecyl sulfate (SDS) loading

buffer (4X) (Appendix 2) and boiled at 70°C for about 10 minutes. Next, 25-50 µg of the protein samples, with equal protein concentration, was loaded on to 3-8% SDS-polyacrylamide gels or 4-12% Bis-Tris Mini gels (both from Life Technologies) with PageRuler prestained protein ladder (Thermo Fisher Scientific) and run in Novex electrophoresis chambers (Life Technologies). The protein gel, filter paper (Bio-Rad), polyvinylidene fluoride (PVDF) membrane (Millipore) were all soaked in transfer buffer (Appendix 2) before oriented in the transfer apparatus (Bio-Rad) in the following order from anode to catode: Filter paper, PVDF membrane, protein gel and filter paper. Electrotransfer of proteins from the gel to the PVDF membrane was done at 250 mA per gel per hour. The blot was blocked with 5% nonfat dried milk (AppliChem) and 0.05% Tween 20 in Tris-buffered saline (TBS-T) (Medicago) for 1-2 hours and then incubated with primary antibodies in 5% milk and 0.05% TBS-T overnight at 4°C. After washing with TBS-T, the blot was incubated with secondary antibodies in 5% milk and 0.05% TBS-T for 1-2 hours at room temperature.

The following primary antibodies were used: Anti-TNKS1/2 (rabbit IgG, 1:500, Santa Cruz), anti-AXIN1 (rabbit IgG, 1:1000, Cell Signaling), anti-AXIN2 (rabbit IgG, 1:1000, Cell Signaling), anti-non-phospho (active) β-catenin (rabbit IgG, 1:5000, Cell Signaling), anti-β-catenin (total) (mouse IgG, 1:10000, BD Transduction Laboratories™), anti-phospho-GSK-3β (Ser9) (rabbit IgG, 1:1000, Cell Signaling), anti-GSK-3β (total) (rabbit IgG, 1:1000, Cell Signaling), anti-phospho-AMPKα (Thr172) (rabbit IgG, 1:1000, Cell Signaling), anti-AMPKα (total) (mouse IgG, 1:500, Cell Signaling), anti-phospho-AKT (Ser473) (rabbit IgG, 1:1000, Cell Signaling), anti-AKT (total) (rabbit IgG, 1:1000, Cell Signaling), anti-phospho-mTOR (Ser2448) (rabbit IgG, 1:1000, Cell Signaling), anti-mTOR (total) (rabbit IgG, 1:1000, Cell Signaling), anti-phospho-p70 S6 kinase (Thr389) (rabbit IgG, 1:1000, Cell Signaling), anti-p70 S6 Kinase (total) (rabbit IgG, 1:1000, Cell Signaling), anti-phospho-RPS6 (Ser240/244) (rabbit IgG, 1:1000, Cell Signaling), anti-RPS6 (total) (rabbit IgG, 1:1000, Cell Signaling), and anti-ACTIN (rabbit IgG, 1:1000, Sigma Aldrich). The following secondary antibodies were used: Donkey anti-rabbit IgG-horseradish peroxidase (HRP) and donkey anti-mouse IgG-HRP (both 1:5000, Santa Cruz Biotechnology). Protein bands were visualized using ECL prime (GE Healthcare Amersham) and a ChemiDoc Touch Imager System (Bio-Rad). The composition of buffers and solutions used in the Western blot analysis is given in Appendix 2.

4 Results

4.1 Part 1: Mouse ESCs

To be able to investigate molecular mechanisms involving, the WNT signaling pathway and the AKT/mTOR signaling pathway, in early differentiation of mouse ESCs, a differentiation protocol needed to be established. Furthermore, two mouse ESC lines were selected for this study: Wild-type mouse ESCs and mouse ESCs with double knockout of *Axin1* $^{\Delta/\Delta}$*/Axin2* $^{\Delta/\Delta}$, in order to explore the mechanistic role of AXIN1/2 in driving differentiation. Both the wild-type ESCs and *Axin1* $^{\Delta/\Delta}$*/Axin2* $^{\Delta/\Delta}$ mutant ESCs were tested for pluripotency. Subsequently, two approaches for establishing a differentiation protocol were tested: The first approach utilized an up-regulation of WNT signaling to induce primitive streak formation. The second approach was about testing whether removal of key external factors, necessary for mouse ESC pluripotency, could induce mouse ESC differentiation toward the neuroectodermal lineage. For the protocol establishment, only wild-type ESCs were used.

4.1.1 Validation of mouse ESC pluripotency

To demonstrate the pluripotency of the wild-type mouse ESCs and the *Axin1* $^{\Delta/\Delta}$*/Axin2* $^{\Delta/\Delta}$ mutant mouse ESCs, three tests were performed: i) Alkaline phosphatase staining, ii) gene expression analysis of the main pluripotent markers *Oct4*, *Nanog* and *Sox2*, and iii) immunostaining for OCT4, NANOG and SOX2.

Results from alkaline phosphatase staining (Figure 9) indicated that both the wild-type ESCs and the *Axin1* $^{\Delta/\Delta}$*/Axin2* $^{\Delta/\Delta}$ mutant ESCs had high levels of alkaline phosphatase expression as they appeared red and purple, suggesting that they were pluripotent.

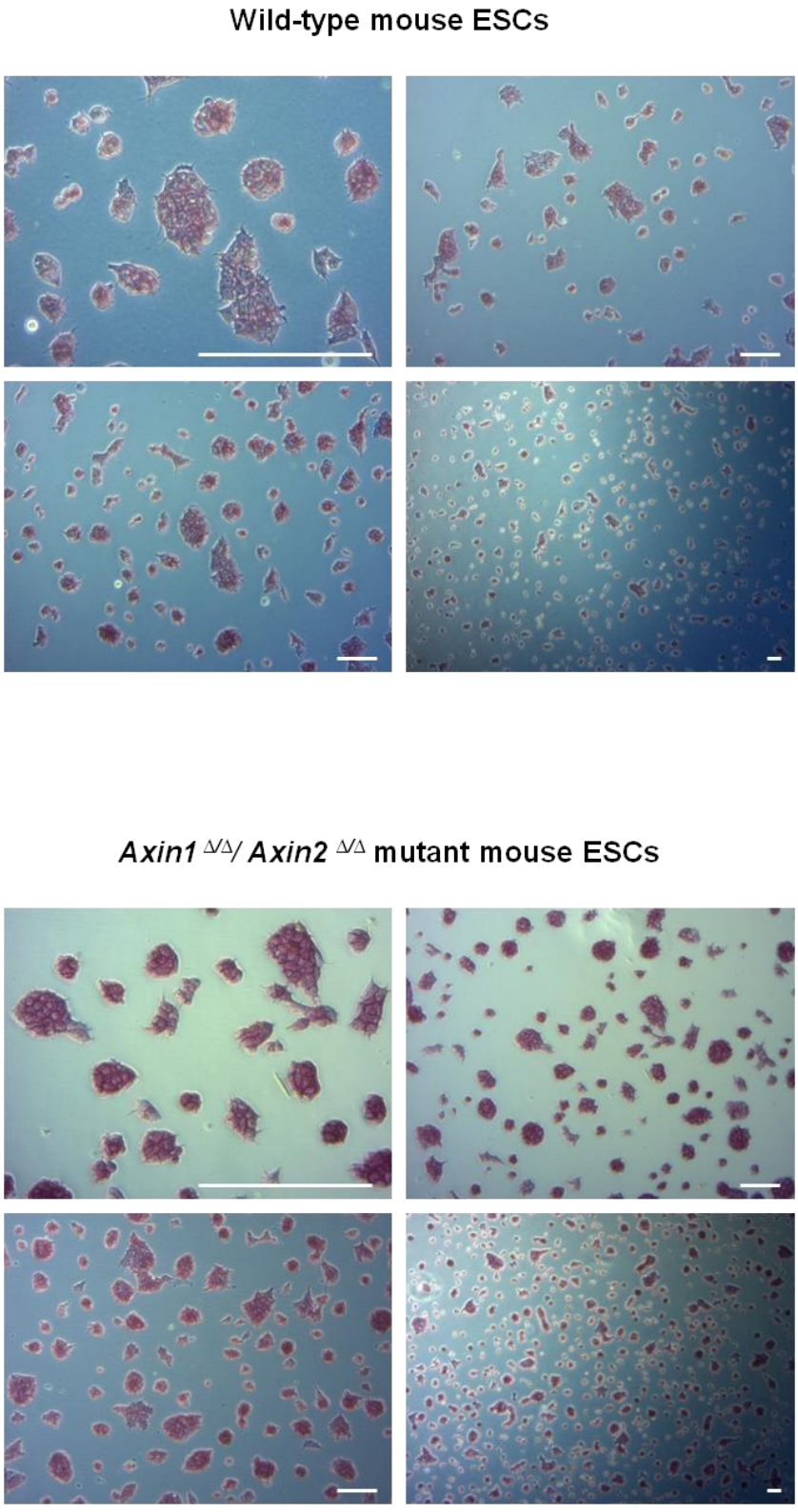

Figure 9. Alkaline phosphatase staining of the mouse ESC lines. Both wild-type mouse ESCs and *Axin1* $^{\Delta/\Delta}$/*Axin2* $^{\Delta/\Delta}$ mutant ESCs appeared purple, indicating high intracellular activity of alkaline phosphatase. The cells were imaged using a phase contrast microscopy. Scale bars, 100 μm.

The gene expression analysis of the main pluripotent marker genes *Oct4*, *Nanog* and *Sox2*, was performed by qRT-PCR. Expression of all the three markers was detected in both the wild-type ESCs and the *Axin1* $^{\Delta/\Delta}$*/Axin2* $^{\Delta/\Delta}$ mutant ESCs, demonstrating their pluripotency (Figure 10).

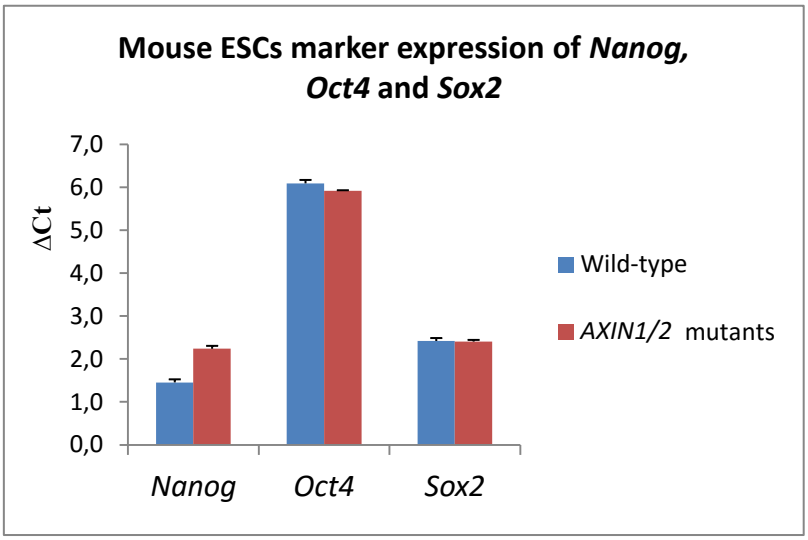

Figure 10. Gene expression levels of *Nanog*, *Oct4* and *Sox2* in both wild-type ESCs (blue) and *Axin1* $^{\Delta/\Delta}$*/Axin2* $^{\Delta/\Delta}$ mutant ESCs (red). The x axis represents the three different markers *Nanog*, *Oct4* and *Sox2*. The y axis represents the ΔC_t values from the qRT-PCR analysis.

Expression of the three key pluripotent markers was further validated by immunochemistry. The wild-type ESCs and the *Axin1* $^{\Delta/\Delta}$*/Axin2* $^{\Delta/\Delta}$ ESCs showed intense immunostaining for OCT4, SOX2 and NANOG (Figure 11), thus demontrating that they were pluripotent and had ESC potential.

Together, these result suggested that the wild-type mouse ESCs and the *Axin1* $^{\Delta/\Delta}$*/Axin2* $^{\Delta/\Delta}$ mutant mouse ESCs were pluripotent with the potential to self-renew.

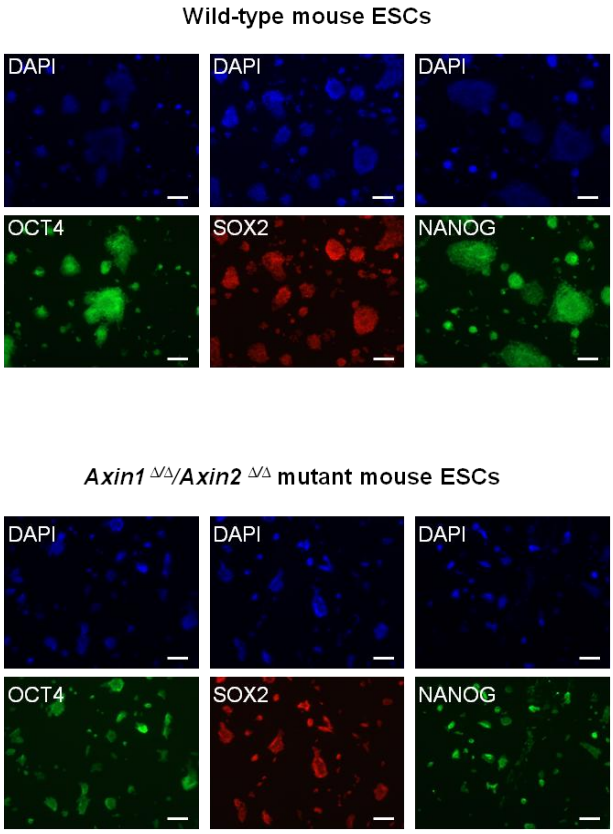

Figure 11. Immunostaining validating gene expression of *Oct4* (green), *Sox2* (red) and *Nanog* (green) in both the mouse ESC lines. The wild-type ESCs and the *Axin1* $^{\Delta/\Delta}$/*Axin2* $^{\Delta/\Delta}$ mutant ESCs were immunostained for OCT4, SOX2 and NANOG. Blue staining represents DAPI staining of total nuclei of. The cells were imaged using a fluorescent microscopy. Scale bars, 100 µm.

4.1.2 Differentiation of the mouse ESCs

Induction of primitive streak differentiation by WNT3A treatment

The first approach to establish a mouse ESC differentiation protocol was based on following a published differentiation procedure [8]. This procedure utilizes WNT3A to induce primitive streak. First, the wild-type mouse ESCs were cultured in three different mediums (Knockout DMEM, IMDM and RPMI Medium 1640 with GlutaMAX) supplemented with 50 ng/ml of WNT3A for 3 days. Due to high cell death, qRT-PCR could not be performed, therefore data are not shown. Next, the wild-type mouse ESCs were cultured in the same chemically defined differentiation serum-free medium (ESF basal medium) that was used in the published

procedure [8]. The medium was supplemented with 50 ng/ml of WNT3A and the treatment lasted for 3 days. During the treatment, clear changes in the cells' morphology appeared; the cells shifted from a dome-like, pluripotent morphology (day 0) to a flattened monolayer morphology with bright clusters (day 1 - 3) (Figure 12), suggesting that WNT3A had induced differentiation toward primitive streak. However, the expression levels of marker genes specific for primitive streak and later differentiation stages (mesoderm and endoderm), analyzed by qRT-PCR, showed that no directed differentiation had occurred (Figure 13). Although the expression levels of the two pluripotency markers *Nanog* and *Sox2* were clearly down-regulated, no up-regulation of the relevant primitive streak markers (*T, Mixl1*and *Gsc*) or the mesendoderm and definitive endoderm marker (*Foxa2*) was detected (Figure 13). In addition, no up-regulation was detected for the neuroectoderm marker *Sox1* (Figure 13). The only marker that did show an effect of the WNT3A treatment was the neuroectoderm marker *Zic1* (Figure 13). Combined, these results demonstrated that treating the wild-type mouse ESCs with WNT3A did not induce a reliable differentiation toward a primitive streak stage.

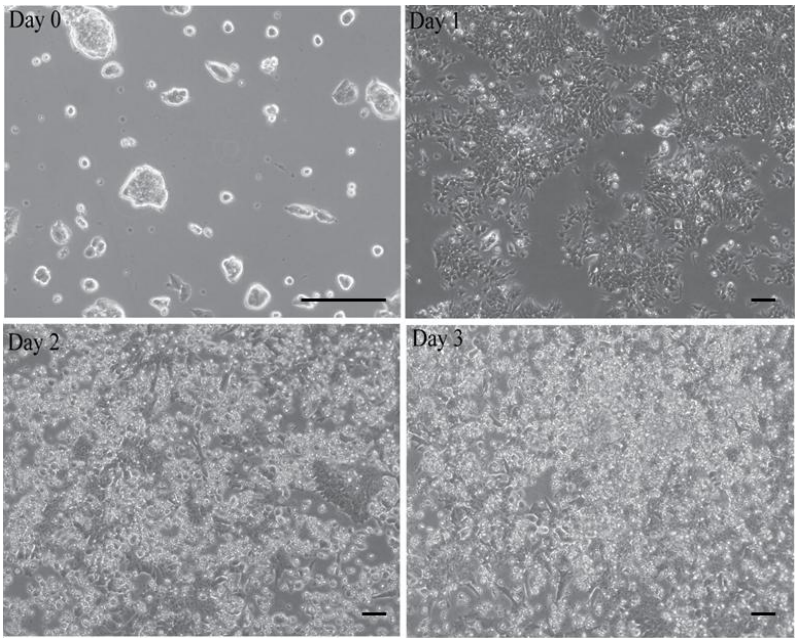

Figure 12. Representative morphology of mouse ESCs (wild-type) observed at different stages after the start of the WNT3A treatment. Day 0 represents untreated mouse ESCs cultured in 2i medium before culturing them in a chemically defined differentiation medium, ESF basal medium, supplemented with 50 ng/ml of WNT3A for 3 days. The cells were imaged using a phase contrast microscopy. Scale bars, 50 µm

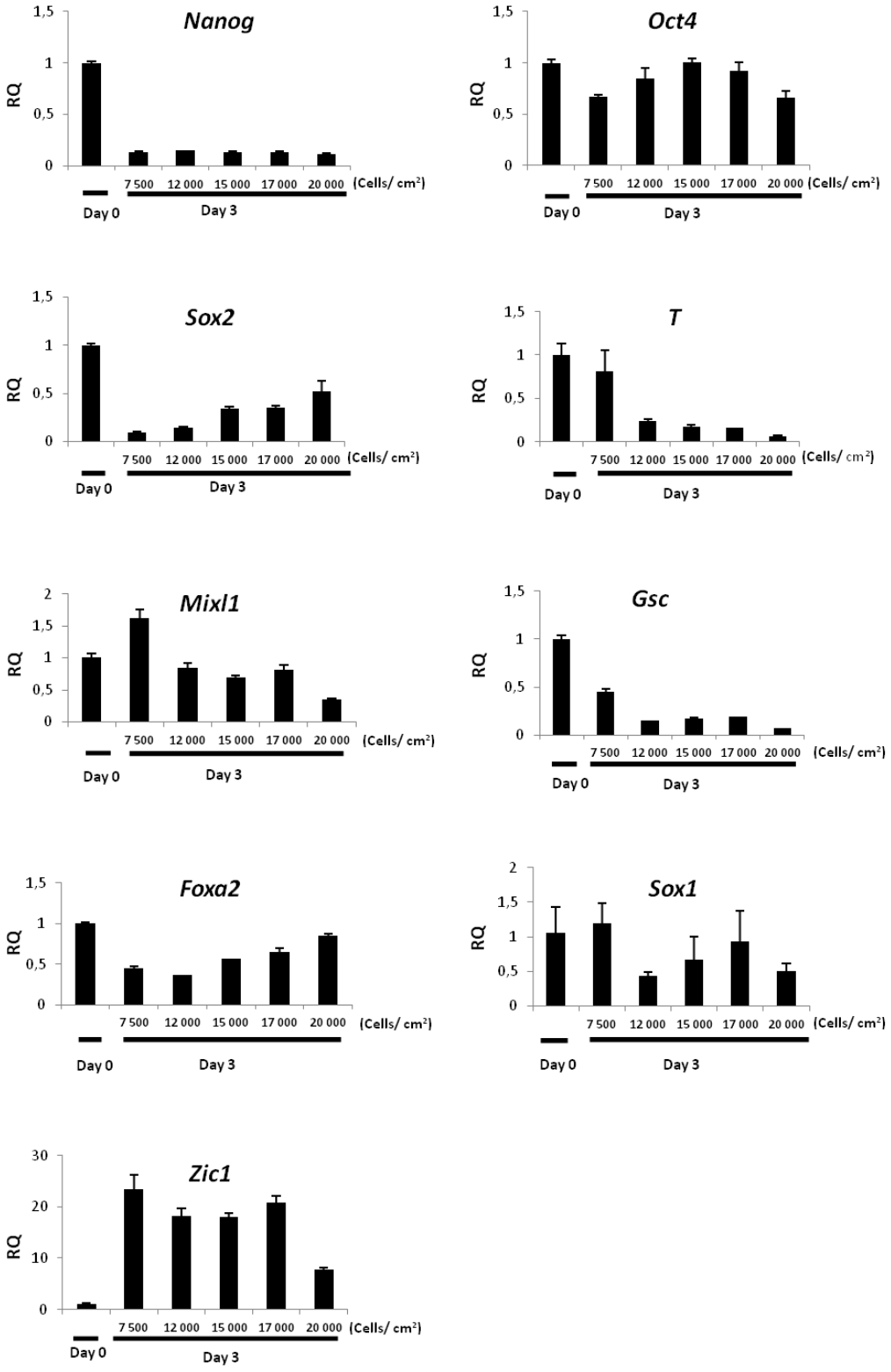

Figure 13. Quantitative analysis of marker gene expression. Mouse ESCs were cultured in ESF basal medium supplemented with 50 ng/ml of WNT3A for 3 days. The expression levels of the relevant markers of primitive streak (*T*, *Mixl1* and *Gsc)*, mesendoderm and definitive endoderm (*Foxa2*) were analyzed by qRT-PCR. The x axis represents the seeding density and days after the start of the treatment. The y axis represents the relative quantification (RQ) values from the qRT-PCR analysis. In all the qRT-PCR graphs, the sample representing day 0 is set to 1, and all other samples are set relative to this sample.

4.1.3 Induction of differentiation by removal of CHIR99021 and LIF

Since the WNT3A treatment in the first approach for developing a differentiation protocol was unsuccessful, the next approached assessed whether removal of the two key extrinsic factors CHIR99021 (GSK-3β inhibitor) and LIF (STAT3 activator), both critical for maintaining mouse ESC pluripotency, could cause the mouse ESCs to exit their pluripotent state and undergo differentiation toward the neuroectodermal lineage. Therefore, mouse ESCs (wild-type) were cultured without the cytokine LIF or the small molecule inhibitor CHIR99021or both, for 24 and 48 hours. Mouse ESCs cultured in 2i medium (with LIF and CHIR99021) were used as a control.

During the treatment, striking changes in cellular morphology appeared: While the undifferentiated cells (control), cultured in 2i medium, showed a ESC-like morphology having concentric and compact colonies, mouse ESCs cultured without LIF or CHIR99021 or both were growing in spreading and flattened colonies (Figure 14). However, cells cultured without LIF had more compact colonies with more ESC-like morphology compared to the cells cultured without CHIR99021 (Figure 14).

The expression levels of marker genes specific for the neuroectoderm lineage (*Sox1* and *Zic1*) were analyzed by qRT-PCR. To make sure that there had been no differentiation toward the mesoderm and endoderm lineages, expression levels of relevant markers of primitive streak (*T, Mixl1* and *Gsc*) were monitored. The results revealed that none of the expression levels of the lineage specific markers had been up-regulated after removing LIF or CHIR99021 for 24 and 48 hours (Figure 15). Furthermore, no dramatic change in the expression level of the pluripotent marker *Sox2* was detected, whereas the expression levels of *Nanog* and *Oct4* were slightly decreased (Figure 15).

In summary, removing LIF and CHIR99021 from the medium was an insufficient method for targeted differentiation of the wild-type mouse ESCs toward a neuroectodermal lineage. Thus, none of the approaches to establish a differentiation protocol for the mouse ESCs worked. Therefore, due to limited time, further analyses of these cells were discontinued.

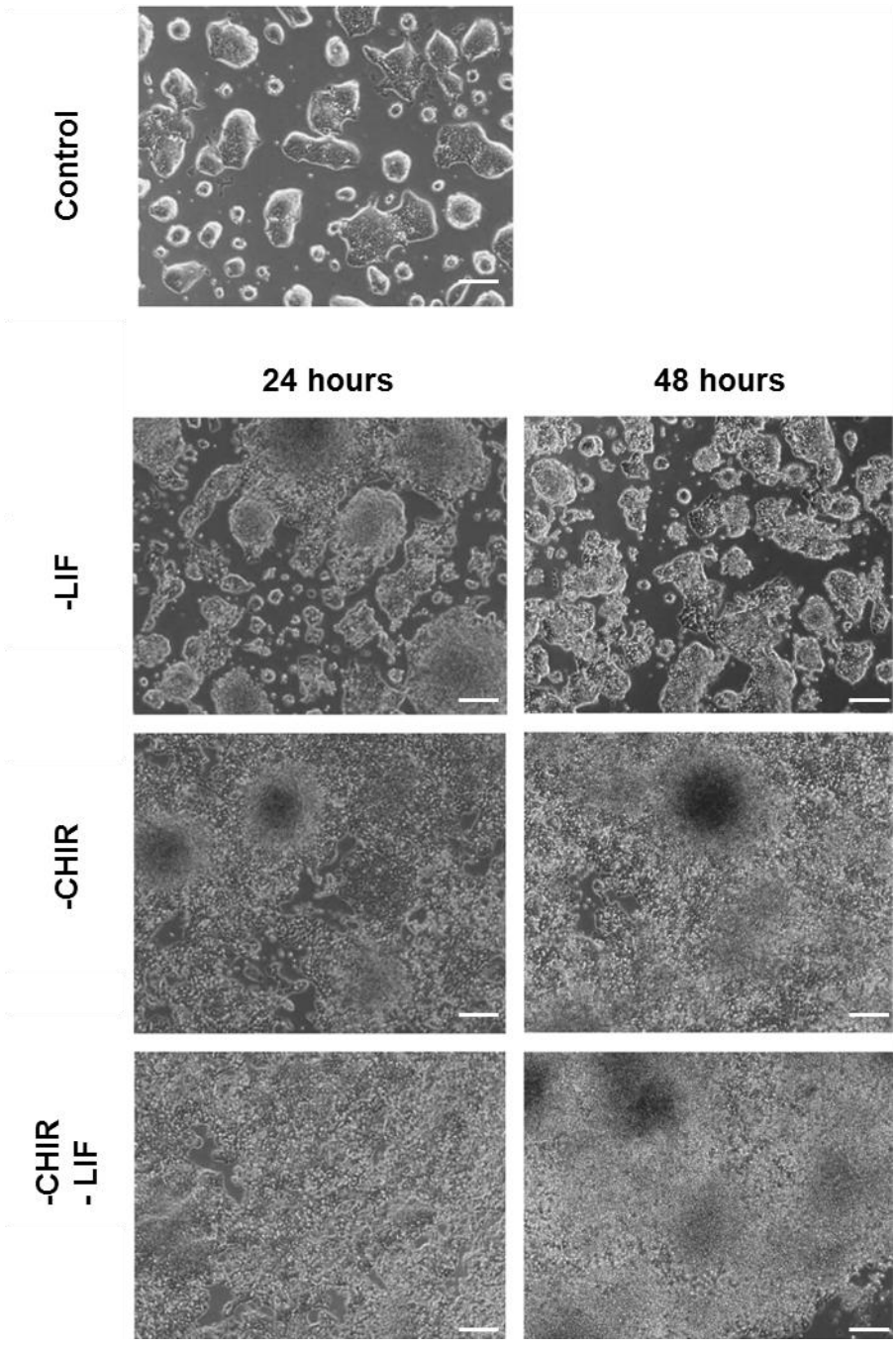

Figure 14. Comparison of representative morphology of i) mouse ESCs grown in 2i medium (control) and ii) mouse ESCs cultured in 2i medium without LIF and iii) mouse ESCs cultured in 2i medium without CHIR99021 and iv) mouse ESCs cultured in 2i medium without LIF and CHIR99021. Cells were collected for analysis 24 and 48 hours after the start of the removal of LIF and CHIR99021. The cells were imaged using a phase contrast microscopy. Scale bars, 100 µm.

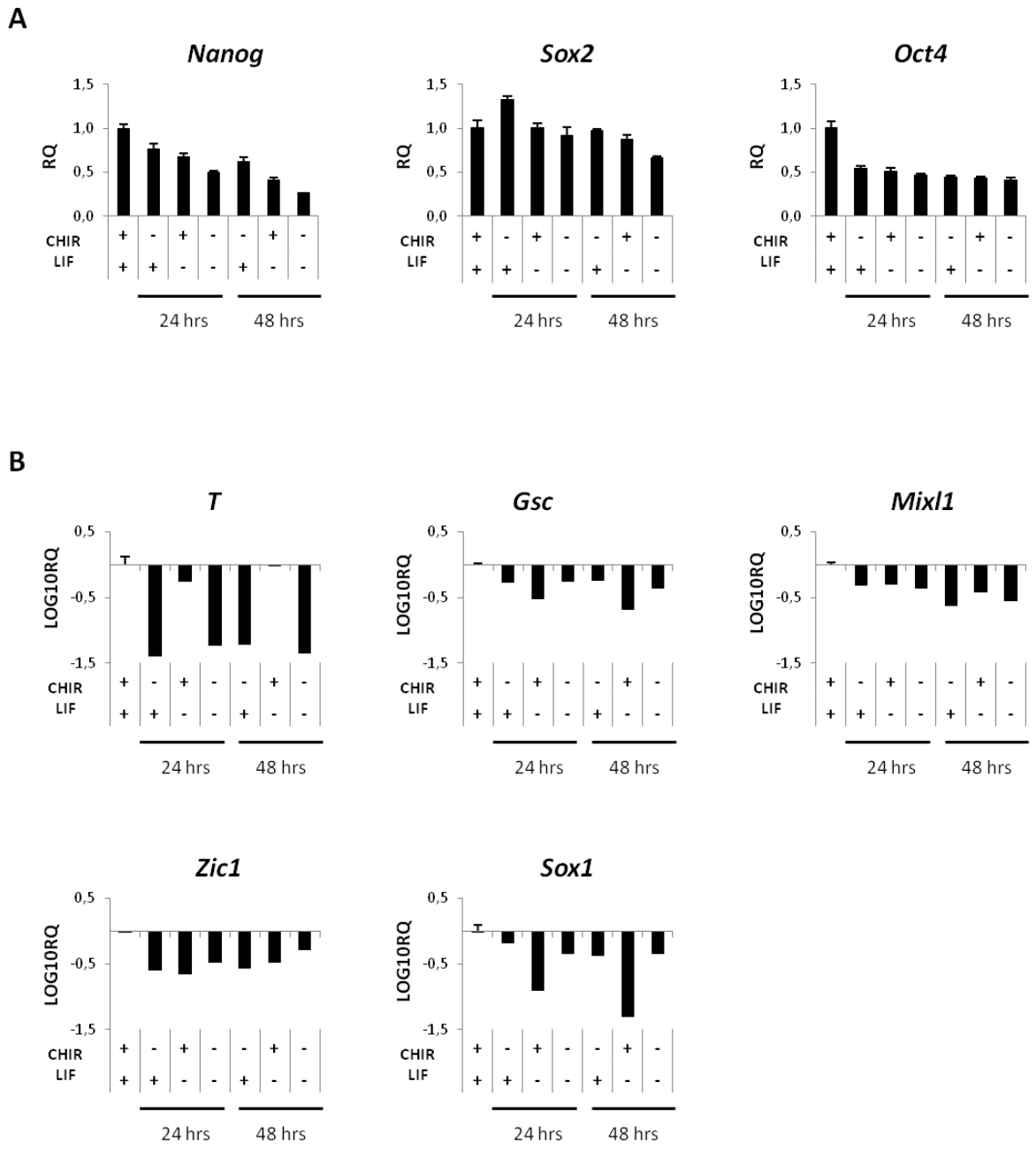

Figure 15. Quantitative analysis of marker gene expression. Mouse ESCs were cultured in 2i without LIF or CHIR99021 or both for 24 and 48 hours. Mouse ESCs grown in 2i (with CHIR99021 and LIF) were used as a control. (A) Expression levels of the pluripotency markers (*Nanog*, *Sox2 and Oct4)*. The x axis represents the three different culture conditions and the two different time points (24 and 48 hours) when cells were collected for analysis. The y axis represents the relative quantification (RQ) values from the qRT-PCR analysis. (B) Expression levels of relevant markers of neuroectoderm (*Zic1* and *Sox1*) and primitive streak (*T, Gsc* and *Mixl1*). The x axis represents the three different culture conditions, and the two different time points (24 and 48 hours) when cells were collected for analysis. The y axis represents the log10 relative quantification (RQ) values from the qRT-PCR analysis. In the qRT-PCR graphs of the expression levels of *Nanog*, *Sox2* and *Oct4*, the sample representing the control is set to 1, and all other samples are set relative to this sample. In the qRT-PCR graphs of the expression levels of the differentiation markers (*T, Gsc, Mixl1, Zic1* and *Sox1*) the sample representing the control is set to 0, and all other samples are set relative to this sample.

4.2 Part2 : Human ESCs

4.2.1 Investigation of the WNT and AKT/mTOR signaling pathways in early differentiation of human ESCs

Aiming at studying the molecular mechanisms of how the WNT and AKT/mTOR signaling pathways and their signaling crosstalk are implicated in early human ESC differentiation, the human ESC line H1 was differentiated following a well-established endodermal differentiation procedure [9]. This procedure utilizes GSK-3β inhibition to prime human ESCs for differentiation into definitive endoderm.

First, the human ESCs were cultured in RPMI-B27 supplemented with 3 µM of CHIR99021 (GSK-3β inhibitor) for 24 hours. Second, they were exposed to a non-primed differentiation using RPMI-B27 alone for another 24 hours (Figure 16). The transition between these two different culture conditions represents the critical cell-fate decision point.

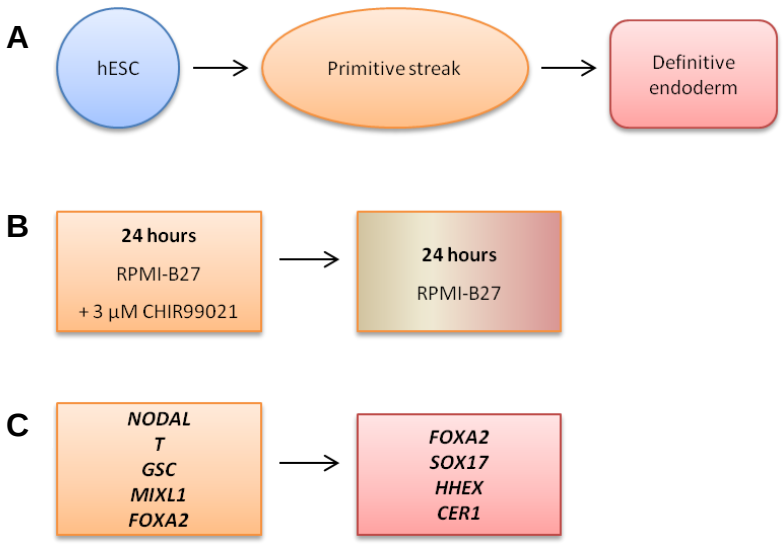

Figure 16. Schematic of the differentiation process. (A) The different stages that human ESCs pass through during endodermal differentiation. First, human ESCs are directed to form a primitive streak population and then the differentiation proceeds toward definitive endoderm. (B) Overview of the culturing conditions used for priming the human ESCs for endodermal differentiation. (C) Key gene expression markers for primitive streak (orange) and definitive endoderm (red) [9].

Over the 48-hour time period, increased expression of definitive endoderm markers such as *FOXA2, SOX17, HHEX* and *CER1* was observed (Figure 17), indicating a successful endodermal differentiation. In addition, there was a rapid up-regulation of *NODAL* within 4 hours followed by an elevated expression of *T* and *GSC* indicating that the cells had passed through primitive streak (Figure 17). Interestingly, the expression profiles of nearly all the markers changed in a biphasic manner: Up-regulated expression at 4 hours, downregulated expression at 8 hours and then a gradual up-regulation again at 12 - 48 hours. To make sure that there was no differentiation toward ectoderm during the 48-hour time course, gene expression levels of the early neuroectoderm markers *ZIC1* and *PAX6* were analyzed. However, no up-regulated expression of these two markers was observed (Figure 17). These changes in gene expression were consistent with the observed morphological changes; the cells shifted from a typical pluripotent morphology (Figure 18A) to dens bright clusters after 24 hours (primitive streak-like morphology), followed by a petal-like morphology after 48 hours (Figure 18B), demonstrating endoderm formation.

To explore the molecular mechanisms in the WNT and AKT/mTOR signaling pathways during the differentiation process, a Western blot analysis was performed for key components of the pathway. Notably, the abundance of almost all the proteins and protein modifications (phospho-AMPKα, phospho-GSK-3β, TNKS1/2, AXIN1/2, active and total β-catenin, and phospho- and total p70S6K) (Figure 21A and 21B, left panel, page 47) changed biphasically in a manner similar to that observed for the expression of the marker genes (Figure 17). Within the first 4 hours there was a rapid up-regulation of the abundance of active and total β-catenin (Figure 21A, left panel), as was expected from the CHIR99021 treatment [9, 128, 129], which lasted for 24 hours until CHIR99021 was removed from the medium. In addition, a rapid up-regulated protein expression of AXIN2 (WNT target gene) was observed after 4 hours (Figure 21A, left panel), indicating that CHIR99021 induced β-catenin-mediated transcriptional activity. Further, AXIN1 and TNKS1/2 were up-regulated within the first 4 hours and then downregulated towards the end (Figure 21A, left panel). Phosphorylation and activation of the important energy sensor AMPK [108] increased at 4 hours, decreased at 8 hours and then increased dramatically again at 48 hours (Figure 21B, left panel). This observation was accompanied by a gradual decrease in the activating phosphorylations of AKT (at Ser473), mTOR (at Ser2448), p70S6K (at Thr389) and RPS6 (at Ser240/244) (Figure 21B, left panel). Combined, these observations suggest that the cells underwent a metabolic shift toward a catabolic state during the differentiation process. With

regard to GSK-3β, a slight decrease in the phosphorylation of GSK-3β at Ser9, rendering it catalytic inactive, was observed after 12 hours (Figure 21B, left panel), which could be due to less active AKT. However, this decrease was followed by an increase after 24 and 48 hours, when the abundance of the active AKT was most reduced (Figure 21B, left panel). Therefore, these results show no clear correlation between active AKT and phosphorylation of GSK-3β at Ser9.

Together, these results demonstrate that the CHIR99021-induced endodermal differentiation triggered stimulation of the WNT signaling pathway (as was expected), activation of AMPK and attenuation of the AKT/mTOR pathway.

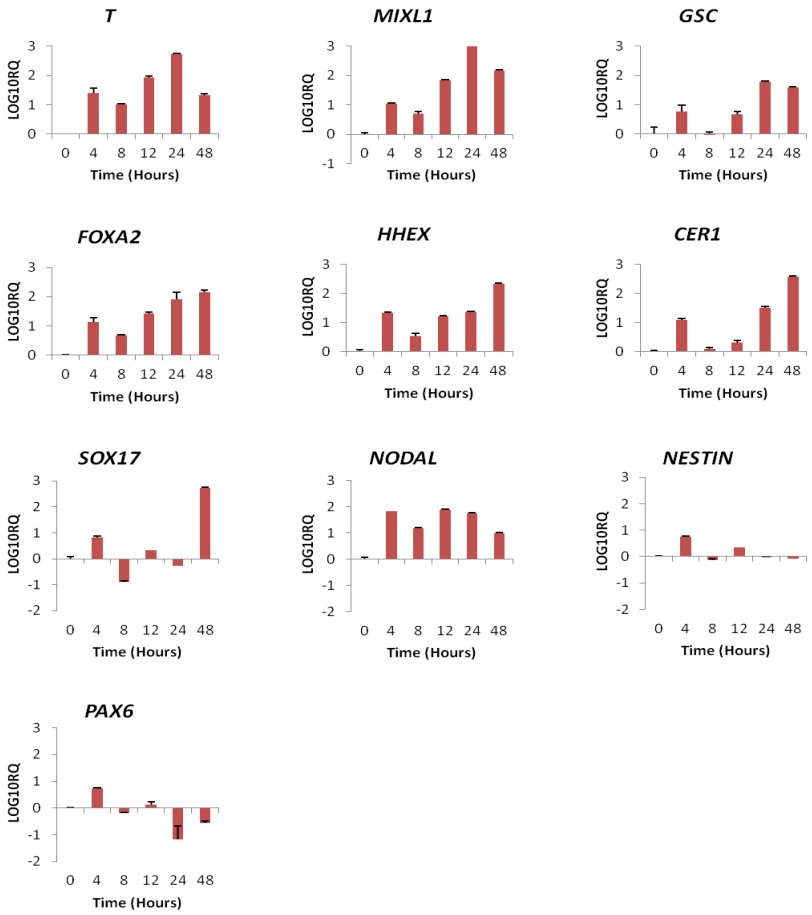

Figure 17. Quantitative analysis of changes in marker gene expression during endodermal differentiation of the human ESCs. The human ESCs were differentiated in RPMI-B27 supplemented with 3 µM of CHIR99021 for 24 hours and then in RPMI-B27 alone for another 24 hours. Developmental changes in expression levels of the relevant markers for primitive streak and mesendoderm (*NODAL*, *T*, *GSC*, *MIXL1* and *FOXA2)* and definitive endoderm (*HHEX*, *CER1*, *SOX17* and *FOXA2*) were analyzed by qRT-PCR. The x axis represents the time (in hours) after the start of the differentiation. The y axis represents the log10 relative quantification (RQ) values from the qRT-PCR analysis. In all the qRT-PCR graphs, the sample representing the 0-hour time point is set to 0, and all other samples are set relative to this sample.

4.2.2 Impact of TNKS1/2 inhibition on the primed endodermal differentiation of human ESCs

After mapping changes in the WNT and AKT/mTOR signaling pathways during endodermal differentiation, the next step in this study was to explore how inhibition of the PARsylating activity of TNKS would affect the CHIR99021-driven differentiation process. First, the human ESCs were treated with 1 µM of G007-LK or 0.11% DMSO (control) while differentiating in RPMI-B27 supplemented with 3 µM of CHIR99021 for 24 hours. Next, the cells were exposed to a non-primed differentiation using RPMI-B27 alone for another 24 hours. During the first 24-hour time period, no obvious differences in the morphological changes were observed between the G007-LK-treated cells and the untreated control cells (0.11% DMSO); both shifted from a pluripotent morphology (Figure 18A) to a dense, bright and clustering morphology after 24 hours (Figure 18B and 18C), suggesting that both had formed primitive streak-like populations and that TNKS inhibition did not antagonize the moving of ESCs from an undifferentiated to a differentiated, primitive streak-like state. However, after the next 24 hours, when both CHIR99021 and G007-LK or DMSO were removed, striking differences were observed: Cells without TNKS inhibition treatment had formed a petal-like morphology typical for definitive endoderm (Figure 18B), whereas G007-LK-treated cells formed dense, irregular and recalcitrant colonies, indicating an unsuccessful differentiation (Figure 18C).

The observed morphological changes were accompanied by changes in the gene expression pattern analyzed by qRT-PCR. Within the first 4 hours, elevated expression of *NODAL* was observed for both the untreated cells and the G007-LK-treated cells (only slightly less) indicating a transition through a primitive streak intermediate (Figure 19). This was followed by an up-regulation of the primitive streak markers *T*, *GSC* and *FOXA2* (Figure 19). However, at the 24-hour time point, expression of *T*, *MIXL1*, *GSC*, *HHEX* and *CER1* was significantly reduced in the G007-LK-treated cells compared to their untreated control counterparts (Figure 19). This was also observed at the 48-hour time point, in addition to significantly expression reductions of *NODAL* and the two definitive endoderm markers *FOXA2* and *SOX17* (Figure 19). Interestingly, expression of the early neuroectoderm marker *PAX6* was significantly higher in the treated cells at the 48-hour time point than in the untreated control cells (Figure 19), whereas there was no significant difference in the expression of the other neuroectoderm marker *NESTIN* (Figure 19).

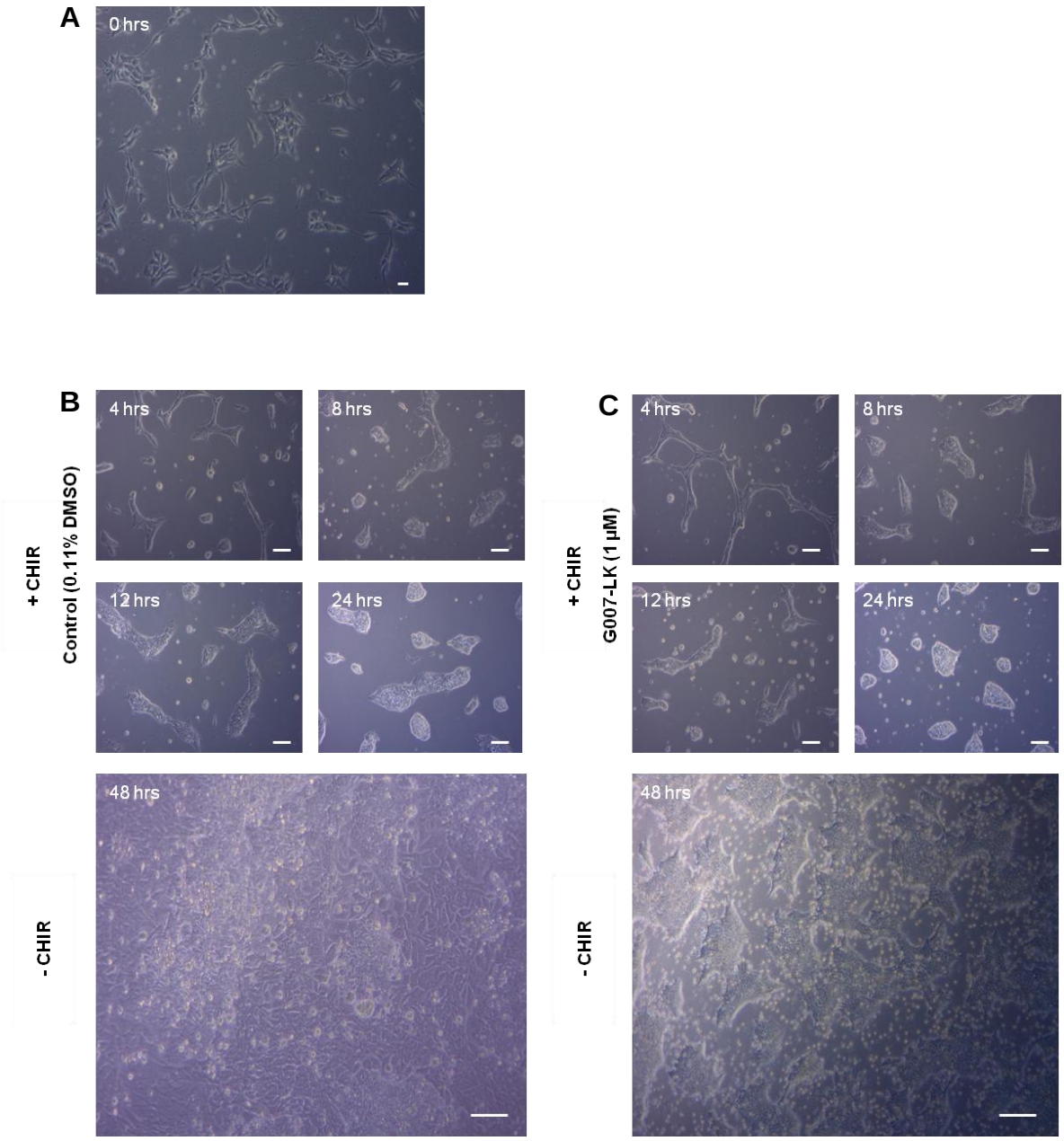

Figure 18. Morphological comparison of differentiating untreated human ESCs (control) and human ESCs treated with G007-LK. (A) Representative morphology of undifferentiated human ESCs 0 hours after the start of the differentiation. Scale bars, 100 µm. (B) Representative morphology of differentiating untreated control human ESCs (0.11% DMSO) observed at each time point, 4, 8, 12, 24, and 48 hours after the start of the differentiation. CHIR99021 and DMSO were removed from the medium after 24 hours. Scale bars, 100 µm. (C) Representative morphology of differentiating human ESCs treated with 1 µM of G007-LK observed at the same time points as the untreated control cells. CHIR99021 and G007-LK were removed from the medium after 24 hours. Scale bars, 100 µm. All cells were imaged using a phase contrast microscopy.

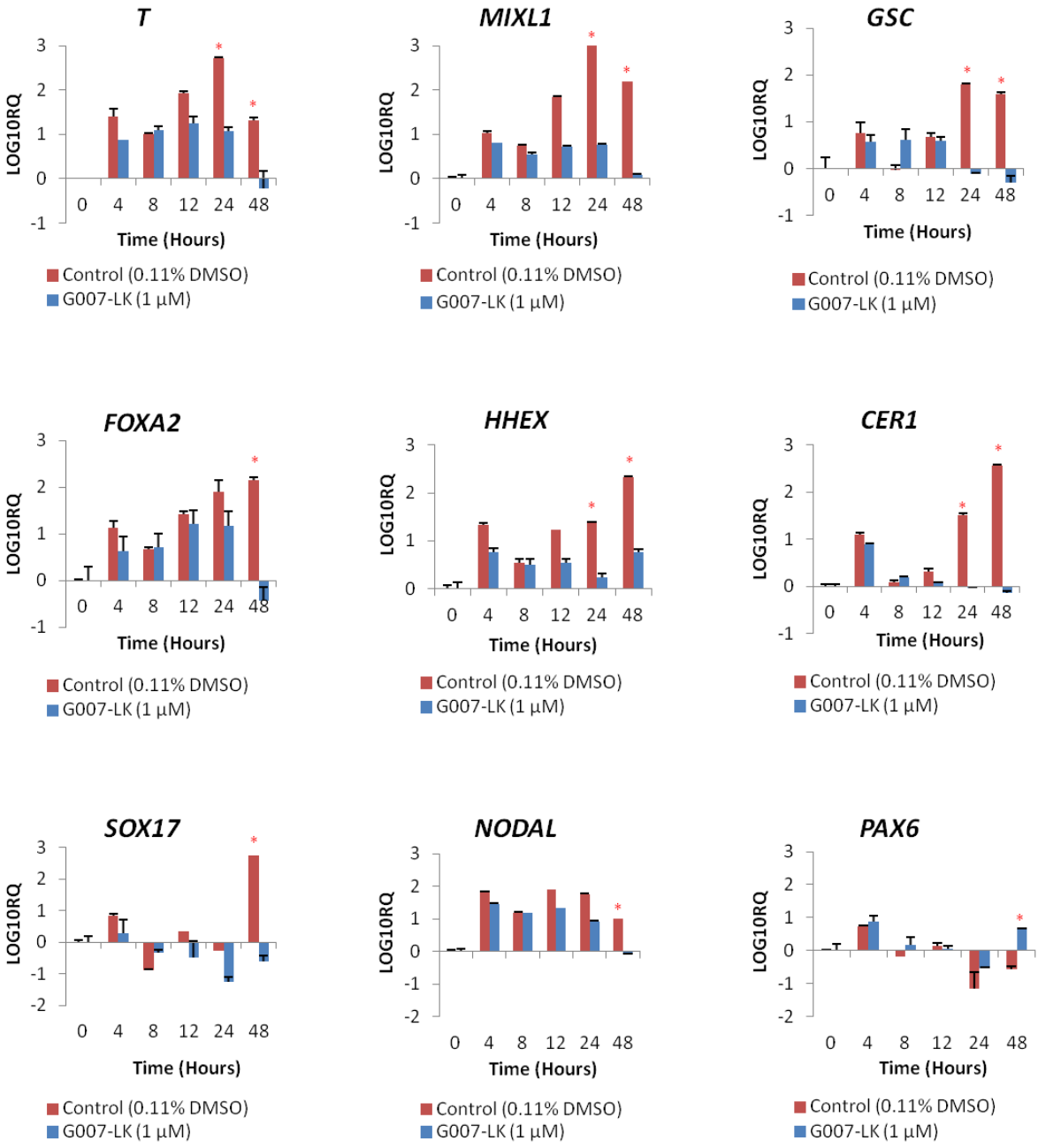

Figure 19. Comparison of the developmental changes in marker gene expression, analyzed by qRT-PCR, during differentiation of the human ESCs treated with 1 µM of G007-LK and the untreated control human ESCs. Untreated control cells (red) were cultured in RPMI-B27 supplemented with 3 µM of CHIR99021 and 0.11% DMSO. Treated cells (blue) were cultured in RPMI-B27 supplemented with 3 µM of CHIR9902 and 1 µM of G007-LK. CHIR99021, G007-LK and DMSO were removed from the medium after 24 hours. The x axis represents the time (in hours) after the start of the differentiation. The y axis represents the log10 relative quantification (RQ) values from the qRT-PCR analysis. In all the qRT-PCR graphs, the sample representing the 0-hour time point is set to 0, and all other samples are set relative to this sample. * represents statistical significant difference ($P<0.01$) between untreated control cells and treated cells upon calculation with the Student t-test. The experiment was repeated twice.

To examine the effects of CHIR99021 alone (in untreated cells) versus CHIR99021 in combination with G007-LK (in treated cells) on the transcriptional activity of β-catenin, changes in expression levels of *AXIN2* during the differentiation were monitored by qRT-PCR. In the cells without G007-LK treatment, there was a clear CHIR99021-mediated up-regulation of *AXIN2* gene expression (Figure 20). This increased expression level changed in a biphasic manner: A rapid up-regulation within 4 hours, followed by a decline at 8 hours, then an increase at 12 hours and then a final gradual decrease to the basal level at 48 hours (Figure 20). In contrast, in G007-LK-treated cells, the effect of CHIR99021 was counteracted by G007-LK; the expression of *AXIN2* was significantly reduced during the differentiation process, even after the 24-hour time point, when both CHIR99021 and G007-LK were removed from the medium (Figure 20). Hence, G007-LK treatment reduced the level of the transcriptional activity of β-catenin and *AXIN2* expression in the context of CHIR99021 induced differentiation (Figure 20).

In conclusion, these results suggest that TNKS1/2 inhibition, in conjunction with GSK-3β inhibition, allowed the cells to reach a primitive streak like intermediate during the first 24 hours of development, but disenabled a transition to a definitive endoderm differentiation after the decision point at 24 hours.

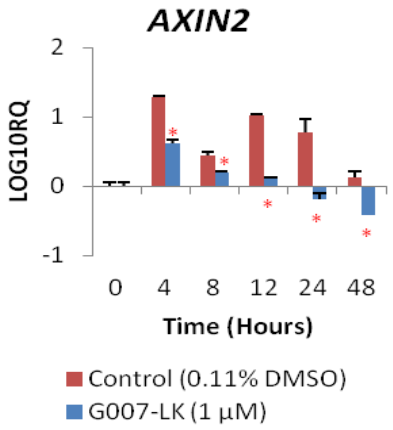

Figure 20. Comparison of the changes in *AXIN2* gene expression during the differentiation of G007-LK-treated cells and untreated control cells. Untreated human ESCs (red) were cultured in RPMI-B27 supplemented with 3 µM of CHIR99021 and 0.11% DMSO. G007-LK-treated human ESCs (blue) were cultured in RPMI-B27 supplemented with 3µM of CHIR99021 and 1 µM of G007-LK. CHIR99021, G007-LK and DMSO were removed from the medium after 24 hours. The x axis represents the time (in hours) after the start of the differentiation. The y axis represents the log10 relative quantification (RQ) values from the qRT-PCR analysis. The sample representing the 0-hour time point is set to 0, and all other samples are set relative to this sample. * represents statistical significant difference ($P<0.01$) between untreated control cells and treated cells upon calculation with the Student t-test. The experiment was repeated once.

To explore how TNKS1/2 inhibition, in the context of GSK-3β inhibition-induced differentiation, affected central proteins in the WNT and AKT/mTOR signaling pathways, a Western blot analysis was performed. For this analysis, 1 additional sample of cells treated with G007-LK for 48 hours, not just 24 hours, (*sample+, 48h**) was made in order to investigate the molecular effects of maintaining G007-LK in the medium. The other sample of cells was treated with G007-LK for 24 hours (*sample-, 48h*).

In general, G007-LK had impact on nearly all the proteins involved in the WNT and AKT/mTOR signaling pathways, in addition to the phosphorylation status of AMPKα and GSK-3β (Figure 21A and 21B, right panel). Over the 48-hour time period, a clear correlation between TNKS1/2 inhibition and AXIN1/2 stabilization was observed, which corresponds to the predicted effects of G007-LK [56]. Consequently, the levels of both AXIN1 and AXIN2 were higher in the treated cells (Figure 21A, right panel) compared to the untreated control cells (Figure 21A, left panel). In the treated cells, the abundance of AXIN1 increased within the first 4 hours and augmented further gradually until it dropped at 48 hours in *sample-* (*48h*) whereas it remained in *sample+* (*48h**) (Figure 21A, right panel). Similarly, a rapid 4-hour-stabilization was observed for AXIN2. This stabilization remained stable until the 48-hour time point in *sample+* (*48h**), but became counteracted in *sample-* (*48h*) upon G007-LK removal (Figure 21A, right panel). In addition, TNKS1/2 inhibition did also cause a predicted reduction of active β-catenin [56], especially after 12 hours (Figure 21A, right panel). Furthermore, G007-LK led to higher abundance of TNKS1/2 within 4 hours in the treated cells (Figure 21A, right panel) compared to the untreated control cells (Figure 21A, left panel), but this effect was rapidly attenuated. Next, the phosphorylation of GSK-3β at Ser9 was more rapidly reduced after the start of differentiation in the treated cells (Figure 21B, right panel) compared to the untreated control cells (Figure 21B, left panel). In addition, the highly increased phosphorylation of AMPKα in the untreated control cells at 48 hours (Figure 21B, left panel), was equally reduced in both *sample-* (*48h*) and *sample+* (*48h**) representing the G007-LK-treated cells (Figure 21B, right panel). With regard to the AKT/mTOR signaling pathway, increased phosphorylation levels of both AKT (Ser473), mTOR (Ser2448) and RPS6 (Ser240/244) were seen in the G007-LK-treated cells (Figure 21B, right panel) compared to the untreated control cells (Figure 21B, left panel).

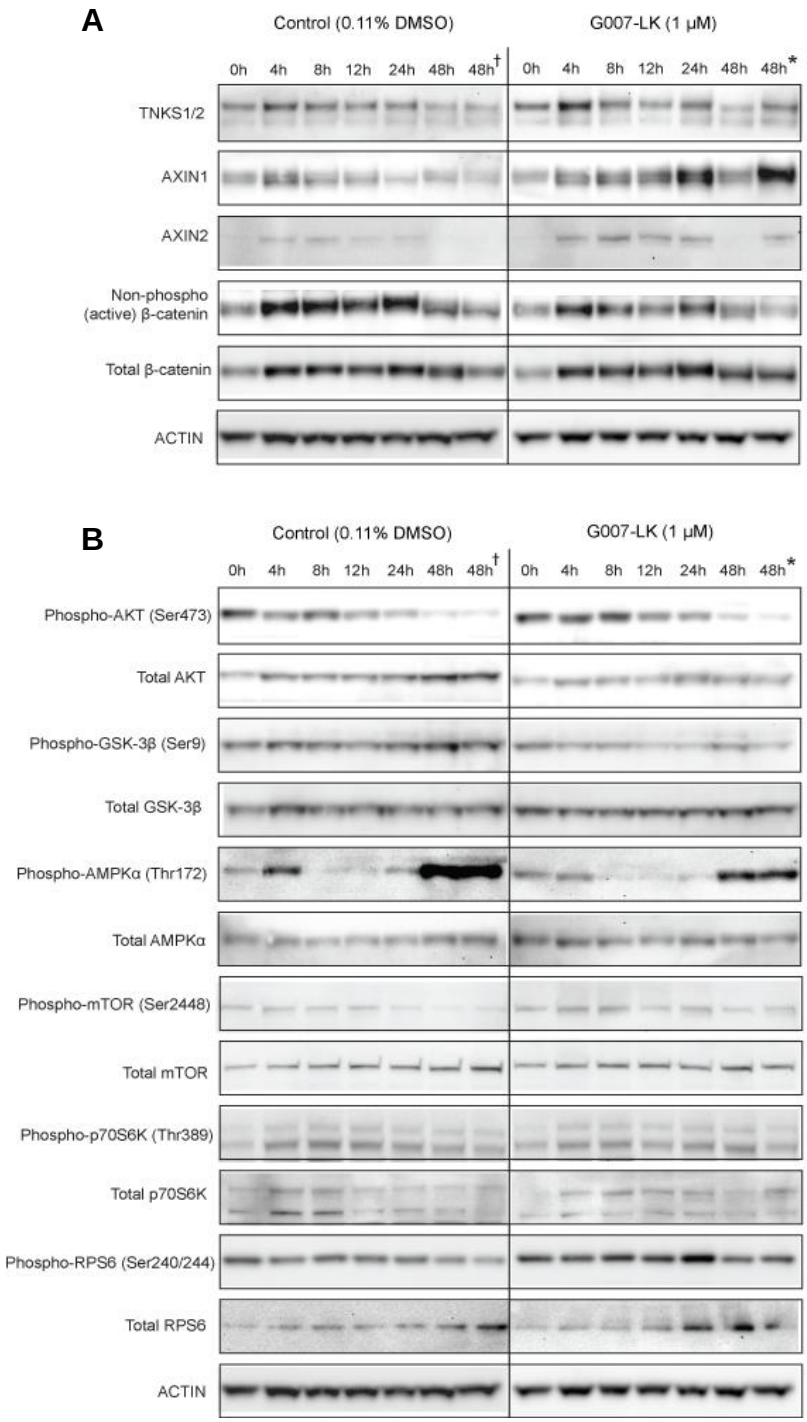

Figure 21. Western blot analysis representing the molecular effects of the G007-LK treatment compared to the control during the endodermal differentiation of the human ESCs. The G007-LK-treated cells (represented in the right panel of the Western blots A and B) were cultured in RPMI-B27 containing 3 µM of CHIR99021 and 1 µM of G007-LK for 24 hours, followed by 24 hours in RPMI-B27 alone or in combination with 1 µM of G007-LK (represented by *). The untreated cells (represented in the left panel of the Western blots A and B) were cultured in RPMI-B27 containing 3 µM of CHIR99021 and 0.11% DMSO for 24 hours, followed by 24 hours in RPMI-B27 alone or in combination with 0.11% DMSO (represented by †). (A) Represents proteins in the WNT signaling pathway in addition to ACTIN. (B) Represents the proteins in the AKT/mTOR signaling pathway in addition to GSK-3β, AMPKα and ACTIN. Cells were collected for analysis 0, 4, 8, 12, 24 and 48 hours after the start of the differentiation. The experiment was repeated twice. Both of the Western blots (A and B) were made from the same cell lysates.

4.2.3 Impact of AKT activation on the primed endoderm differentiation of human ESCs

The last step in this study was to assess whether the observed gradual decrease in active AKT (Ser473 phosphorylation) during the standard endodermal differentiation process (Figure 21B, left panel), could be counteracted by treating the human ESCs with an AKT activator in order to study if this delayed or blocked the formation of endoderm. A pilot experiment was undertaken to find the optimal dose of the AKT activator SC79. The human ESCs were treated for 24 hours with a dose-titration (0, 2, 5, 10, 15 µM) of SC79 or 0.015% DMSO (control) while differentiating in RPMI-B27 with 3 µM of CHIR99021. Unfortunately, over the 24-hour time period, no enhanced Ser473 phosphorylation was detected for any of the selected concentrations of SC79 after the 0-hour time point (Figure 22). Nor did it increase more than the phosphorylation status of AKT in the untreated control cells at 24 hours, observed in the first Western blot analysis (Figure 21B, left panel).

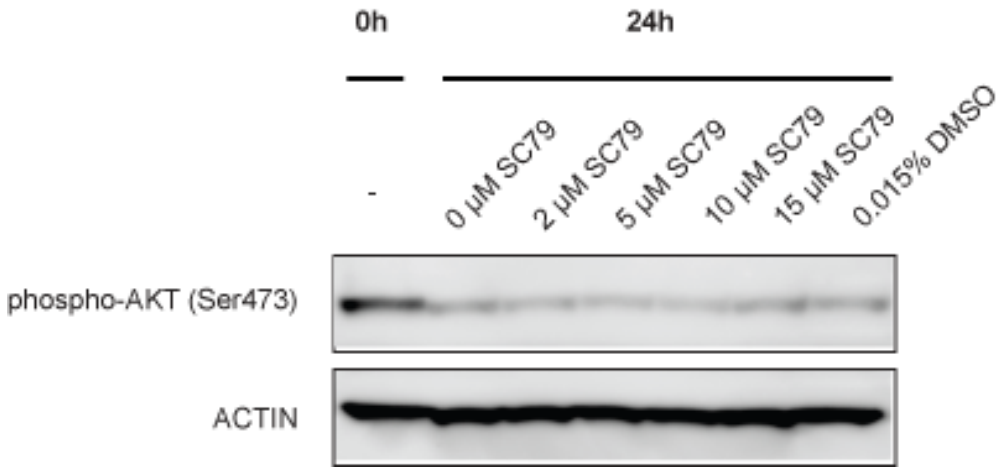

Figure 22. Western blot analysis representing the effects of the SC79 treatment on Ser473 phosphorylation of AKT during endodermal differentiation of the human ESCs. The human ESCs were treated with a dose-titration (0, 2, 5, 10, 15 µM) of SC79 (AKT activator) or 0.015% DMSO (control) for 24 hours while differentiating in RPMI containing 3 µM of CHIR99021. The cells were collected for Western blot analysis 0 and 24 hours after the start of the treatment.

5 Discussion

Changes in both the WNT signaling pathway and the major anabolic pathway AKT/mTOR have previously been linked to the early transition steps of ESCs from the pluripotent state to lineage commitment [7, 10, 45, 130, 131]. However, the molecular mechanisms of how these two pathways separately, and together, integrate in early differentiation of ESCs are yet not fully understood. This study reveal interesting results demonstrating that the abundance of critical proteins, regulating the WNT and AKT/mTOR pathways, changes in a biphasic manner during endodermal differentiation of human ESCs. Furthermore, the data presented here demonstrate how TNKS1/2 inhibition can counteract the WNT stimulating effect of GSK-3β-inhibition, and also affect AKT/mTOR signaling and the phosphorylation status of GSK-3β and AMPK, thereby blocking the differentiation program. Unfortunately, since the approaches for establishing a mouse ESC differentiation protocol were insufficient, investigation of the WNT and AKT/mTOR pathways in early differentiation of mouse ESCs was not accomplished.

5.1 Validation and differentiation of the mouse ESCs

5.1.1 Validation of the mouse ESCs

Verifying the pluripotency of ESCs, from the establishment of a new cell line to its expansion for an experiment, is a crucial process. ESCs can only be used in a differentiation experiment if they possess the ability to differentiate into any other cell type in the body. Differentiation experiments using invalidated ESC will therefore have low reliability and consistency. Several methods are developed to enable easy ESC verification. To validate the truly pluripotency of the newly generated mouse ESC lines used in this study, three methods were used: Alkaline phosphatase staining, qRT-PCR expression analysis of the main pluripotent markers *Oct4*, *Nanog* and *Sox2* and immunostaining to confirm protein expression of the three pluripotent markers.

Alkaline phosphatase is one of the key markers used for identifying the pluripotency of ESCs derived from both mouse and human [126]. This is based on previous research showing that the inner cell mass has elevated activity of alkaline phosphatase compared to trophoblast cells found in the outer epithelial layer of trophectoderm [126]. On lineage differentiation, the expression of alkaline phosphatase decreases and will only appear in certain specialized cell populations. So far, the specific function and importance of alkaline phosphatase in ESC development, remains poorly understood. One hypothesis has been that ESCs require increased substrate dephosphorylation activity due to an altering and increasing metabolic activity [126]. In this study, both the wild-type mouse ESCs and the *Axin1* $^{\Delta/\Delta}$*/Axin2* $^{\Delta/\Delta}$ mutant mouse ESCs showed high level of alkaline phosphatase expression as they appeared purple upon alkaline phosphatase staining (Figure 9). Thus, both cell lines were pluripotent having the potential to self-renew. Next, qRT-PCR and immunostaining confirmed expression of the three core transcription factors, OCT4, NANOG and SOX2 both at the transcriptional level (Figure 10) and protein level (Figure 11). These three factors are important regulators of the transcriptional network responsible for pluripotency and self-renewal in ESCs and their expression is therefore crucial for maintaining an undifferentiated state [32, 34]. Collectively, these results strongly suggest that these cells were maintained in a pluripotent state.

5.1.2 Differentiation of the mouse ESCs

To be able to study the WNT and AKT/mTOR signaling pathways in early differentiation of mouse ESCs at the molecular level, a differentiation protocol needed to be established. The first approach focused on using a differentiation protocol published in a previous study [8], whereby mouse ESCs were treated with WNT3A for 3 days to induce primitive streak-like cells. During the WNT3A-treatment, striking changes were observed in the cellular morphology, from a pluripotent, doom-like morphology at day 0 to a dense, bright and clustering morphology at day 2 and 3, suggesting that the cells had reached primitive streak (Figure 12) [132]. However, the qRT-PCR data showed no up-regulated expression of the relevant primitive streak differentiation markers (*T, Mixl1* and *Gsc*) or the mesendoderm and definitive endoderm marker (*Foxa2*), even though there were reduced expression of the two pluripotent markers *Nanog* and *Sox2* (Figure 13). To ensure that there had been no

differentiation toward ectoderm, two relevant neuroectoderm makers (*Sox1* and *Zic1*) were monitored. No up-regulation was detected for *Sox1*, whereas the expression of *Zic1*was surprisingly strongly up-regulated (Figure 13). Together, these results indicated that induction of primitive streak had not been achieved. This could have been due, at least in part, to differences between the mouse ESC line C57BL/B6 (B6 mice) used in this study, and the mouse ESC line D3, used in the study where the protocol was published [8]. Furthermore, the mouse ESC line D3 was apparently cultured under serum-free culture conditions prior to differentiation, in order to make the cells more sensitive [133]. In this study, however, the mouse ESC line C57Bl/B6 was cultivated under serum-based conditions. Notably, recent studies have demonstrated that undifferentiated mouse ESCs cultured in serum exhibit high heterogeneity in their gene expression profiles causing intracellular variability. However, this heterogeneity can be reduced using serum-free culture conditions [134, 135]. These findings can therefore partly explain why the mouse ESC line C57Bl/B6 failed to differentiate into the cell type of interest.

The next approach to establish a mouse ESC differentiation protocol explored whether removal of key external factors (LIF and CHIR99021), necessary for maintaining mouse ESC pluripotency, could induce mouse ESC differentiation. Previous research has demonstrated that removal of both LIF and CHIR99021 causes mouse ESCs to exit their pluripotent state and spontaneously undergo neural and ectodermal differentiation [136, 137]. The data revealed in this study, however, are not consistent with these previous findings. Although there were clear morphological changes upon removal of LIF and CHIR99021 in which the cells shifted from a pluripotent morphology to a more spreading and flattened morphology (Figure 14), no elevated expression of the neuroectoderm markers (*Sox1* and *Zic1*) was detected (Figure 15). Nor was there any up-regulation of the primitive streak markers (*T, Gsc* and *Mixl1*) confirming that the cells had not been differentiating into mesoderm or endoderm (Figure 15). With regard to the pluripotency markers, only *Nanog* and *Oct4* were downregulated, whereas the expression of *Sox2* was sustained (Figure 15). Previously, *Sox2* has been identified to be necessary for neuroectodermal differentiation [32, 138] and can be used as an early ectoderm marker [132]. Therefore, it should nonetheless be noted that the mouse ESCs could potentially have been at the earliest stage of a neuroectodermal differentiation and that *Sox1* and *Zic1* then would have been expressed at later time points of the differentiation process.

5.2 Differentiation of the human ESCs

5.2.1 Investigation of the WNT and AKT/mTOR signaling pathways in early differentiation of human ESCs

Investigation of the WNT and AKT/mTOR signaling pathways in early differentiation of human ESCs, was accomplished by following a well-established endodermal differentiation procedure [9]. This procedure utilizes a short pulse (24 hours) of CHIR99021, a small-molecule inhibitor of GSK-3β, to stimulate WNT signaling [9].

The data from the Western blot analysis demonstrated that the abundance of proteins involved in the WNT signaling pathway and the AKT/mTOR pathway, in addition to the phosphorylation status of AMPK and GSK-3β changed in a biphasic manner during the CHIR99021-induced differentiation (Figure 21A and 21B, left panel): A rapid up-regulation at 4 hours, followed by a decrease between 8-24 hours and then either a further decrease (TNKS1/2, active and total β-catenin, phospho-p70S6K (Thr389)) or increase at 48 hours (AXIN1, phospho-AMPKα (Thr172) and phospho-GSK-3β (Ser9)). Interestingly, this biphasic pattern was also observed for the expression profiles of the relevant markers of primitive streak, mesendoderm and definitive endoderm. A possible explanation for the biphasic regulation of the proteins involved in the WNT signaling pathway, comes from a previous study showing that WNT signaling functions biphasically during development and differentiation of ESCs: At early developmental stages, WNT signaling is enhanced to promote differentiation toward definitive endoderm, whereas at later stages, it becomes rapidly inactivated to further promote formation of foregut endoderm [128]. The rapid accumulation of active β-catenin at the protein level confirmed the predicted effects of CHIR99021 (Figure 21A, left panel) [9, 128, 129]. Concomitantly, an increased expression level of the WNT target gene, AXIN2, at both the transcriptional (Figure 20) and protein level (Figure 21A, left panel) further confirmed the predicted induction of WNT/β-catenin-mediated transcriptional activity [128, 129]. This induced transcriptional activity was further rapidly downregulated upon CHIR90021 removal, as judged by the great reduction of AXIN2 at both the transcriptional (Figure 20) and protein level after 24 hours (Figure 21A, left panel). Importantly, all these changes in protein abundance could be effects of the differentiation process, or they could be the main factors inducing the differentiation process.

Previous studies have shown that AXIN2 can function as a direct transcriptional repressor of the WNT target gene *c-MYC* [122], which is involved in inhibiting the conversion of pyruvate to acetyl-CoA [121]. Therefore, based on the observed rapid increase of AXIN2 expression at 4 hours (Figure 20 and 21A, left panel), it is tempting to speculate that AXIN2 is involved in regulating the changes in ESC metabolism during cellular differentiation, which recently have been shown to modulate chromatin plasticity [10, 12, 119, 120]. However, more research is needed to corroborate this hypothesis. One powerful approach to gain a deeper understanding of the role of AXIN2 in differentiation would be to utilize *AXIN2* knockout ESCs.

It has long been known that the AKT/mTOR signaling pathway is involved in receiving signals from nutrients, growth factors and cellular energy status to activate anabolic pathways that stimulate protein, glycogen and lipid synthesis, and cell growth [15, 108, 110]. In contrast, upon metabolic stress and starvation (high AMP/ATP ratio), AMPK gets activated and phosphorylates TSC1, which subsequently inhibits mTOR to prevent glycogen, protein and lipid synthesis [15, 108, 110]. Concomitantly, AMPK stimulates autophagy to degrade macromolecules and organelles in the cytoplasm [10, 108, 110]. The Western blot analysis in this study revealed that phosphorylation and activation of AMPK at Thr172 was highly induced at 48 hours (Figure 21B, left panel). This activation was accompanied by decreased activity of the AKT/mTOR pathway in which the phosphorylations of AKT (at Ser473), mTOR (at Ser2448), p70S6K (at Thr389) and RPS6 (at Ser240/244) were clearly reduced (Figure 21B, left panel). Together, these results suggest that the human ESCs underwent a rapid anabolic-to-catabolic conversion during the differentiation process, which might have led to stimulation of autophagy driven by AMPK-mediated mTOR inhibition. Interestingly, this observation can be linked to previous studies showing that autophagy plays an important role in differentiation of ESCs and embryonic development [10, 13, 139]. As a rapid inducible multistep degradation process, autophagy enables ESCs to recycle internal compounds during their commitment to more specialized cell types with other energetic and biosynthetic requirements [13, 139]. Furthermore, because the AMPK/mTOR pathway regulates mitochondrial biogenesis in somatic cells [10], the observed changes in the abundance of these proteins, during the differentiation, may also indicate changes in the mitochondrial content and functions within the human ESCs. As all these phosphorylation changes were observed during the differentiation process, it is important to point out that further research is needed to find out if these changes are caused by the process or if they are the ones driving the process.

Another interesting implication of the mTOR pathway in ESCs, that could reflect its reduced activity at the end of the endoderm differentiation (Figure 21B, left panel), comes from previous *in vitro* observations demonstrating that inactivation of mTOR with rapamycin disrupts expression of *OCT4, NANOG* and *SOX2* and induces expression of endoderm and mesoderm differentiation genes [131]. Thus, mTOR is involved in regulating the decision point between stem cell maintenance and differentiation.

The mechanism underlying the inhibitory effect of CHIR99021 on GSK-3β involves an interaction with the ATP-binding site of the kinase, which blocks its catalytic activity [140]. Results revealed in a previous study demonstrated that this inhibitory effect does not involve negatively phosphorylation of GSK-3β at Ser9 [141]. However, a Western blot analysis from the same study did show that there was less Ser9 phosphorylation in serum-starved cells treated with CHIR99021 than in serum-starved untreated cells [141]. These findings give additional support to the observations revealed in this study, showing that phosphorylated GSK-3β at Ser9 decreases in the presence of CHIR99021, while it increases upon CHIR99021 removal (Figure 21B, left panel). One possible explanation for this observation is that the binding of CHIR99021 in the ATP pocket [140], may interrupt the phosphorylation of Ser9. Surprisingly, the increase of the negatively Ser9 phosphorylation upon removal of CHIR99021 at 48 hours was apparently not caused by elevated activity of AKT, which is the primary suppressor of GSK-3β (via its Ser9 phosphorylation) (Figure 21B, left panel) [108, 142].

5.2.2 Small molecule-mediated inhibition of TNKS blocks the last phase of endoderm differentiation

Although several studies have revealed new insights into the different molecular mechanisms of TNKS [91, 97, 98], the specific context-dependent function of TNKS in ESC differentiation has not yet been explored. Since TNKS can act as a context dependent gate keeper for WNT/β-catenin signaling, the next aim in this study was to investigate whether the PARsylation activity of TNKS [56, 91], play a role in endoderm differentiation of human ESCs. To accomplish this, the human ESCs were treated with the highly selective TNKS1/2 inhibitor G007-LK for 24 hours, while differentiating toward endoderm, induced by a short pulse of CHIR99021 (24 hours). Interestingly, TNKS inhibition efficiently blocked the last phase of the induced differentiation, as judged by the cells' recalcitrant morphology at 48 hours (Figure 18C) and by the significantly reduced expression levels of all the relevant mesendoderm and definitive endoderm markers at 48 hours (Figure 19). However, G007-LK had almost no effect on the earlier events of the differentiation, during the first 24 hours, in which both the qRT-PCR analysis (Figure 19) and the observed morphological changes (Figure 18C) indicated a normal transition through primitive streak. These observations can partly be explained by the detected changes in *AXIN2* gene expression (Figure 20), demonstrating that the WNT stimulating effect of CHIR99021 was not counteracted by G007-LK until the last 24 hours. Thus, stimulation of WNT/β-catenin signaling was maintained during the first phase of the differentiation, enabling the cells to form the primitive streak.

During gastrulation, ESCs migrate through primitive streak to form either mesoderm or endoderm, whereas the neuroectoderm lineage is formed outside the primitive streak [7, 8]. A recent study demonstrated that human ESC populations having low WNT activity mainly generate neuroectodermal cells with high expression of *PAX6*, whereas WNT high populations primarily form mesoderm or endoderm [7]. These findings are partly consistent with the observations in this study: G007-LK-treated ESCs, having low WNT activity after 24 hours (Figure 20), showed significantly higher expression of the neuroectodermal marker *PAX6* at 48 hours than the untreated control cells with high WNT activity (Figure 19). However, since there was no induced expression of the other neuroectodermal marker *NESTIN* (Figure 19), this result cannot alone indicate that the treated cells, with low WNT activity, formed ectoderm. Furthermore, the expression level of *PAX6* at 48 hours in the treated cells should also have been compared to *PAX6* expression levels in normally formed

ectodermal cells, to assess whether the expression level was significantly high enough to suggest an ectodermal differentiation. Based on these findings and the findings revealed in the previous report [7], it would be interesting to explore how a pre-treatment with G007-LK, making the undifferentiated human ESCs exclusively WNT^{low}, would affect the primed-endodermal differentiation process.

Over the 48-hour differentiation process, there appeared some striking differences in protein levels between the G007-LK-treated cells and their untreated control counterparts (Figure 21A and 21B). First, the treated cells had higher abundance of TNKS1/2 at 4 hours, which gradually attenuated during the 8- and 12-hour time points, and then increased at 24 hours and finally either decreased again at 48 hours in *sample-* (*48h*) or remained stable in *sample+* (*48h**) (Figure 21A, right panel), thus revealing that the level of TNKS1/2 changed biphasically during the differentiation. Secondly, inhibition of TNKS1/2 caused stabilization of AXIN1/2 (Figure 21A, right panel), which is consistent with previous observations [56, 92]. Thus, the level of AXIN1/2 was higher in the treated cells (Figure 21A, right panel) compared to the untreated control cells (Figure 21A, left panel). However, the protein levels of AXIN1 and AXIN2 in the treated cells, during the differentiation, were somewhat different: The abundance of AXIN1 gradually increased as a result of a gradually stronger TNKS1/2 inhibitor effect of G007-LK (Figure 21A, right panel), whereas the abundance of AXIN2 remained stable after the rapid increase at 4 hours (Figure 21A, right panel). This difference can partly be explained by the fact that AXIN2 also is a WNT target gene, as well as being an important component of the β-catenin destruction complex. This was clearly demonstrated in which its gene expression gradually decreased as the effect of G007-LK gradually counteracted the WNT stimulating effect of CHIR99021 (Figure 20). Consequently, up-regulation of AXIN2 within the first hours may not only due to an inhibition of TNKS1/2, but also to the short pulse of CHIR99021, which stimulated transcription of WNT target genes (as was expected) [129]. Thirdly, active β-catenin was decreased at 8-12 hours in the treated cells (Figure 21A, right panel) compared to the untreated controls cells (Figure 21A, left panel). This was also predicted as TNKS inhibition is known to increase the stability of the β-catenin destruction complex, due to the AXIN stabilization, leading to increased proteasomal degradation of β-catenin [56].

As mentioned earlier in the discussion, phosphorylation of GSK-3β at Ser9 decreased in the presence of CHIR99021 during the standard endodermal differentiation (Figure 21B, left

panel). This pattern was also observed during differentiation of the G007-LK-treated cells (Figure 21B, right panel). However, in these cells, there was overall less Ser9 phosphorylation throughout the differentiation process. This might be due to the fact that TNKS inhibition increases the stability of the β-catenin destruction complex, involving GSK-3β [91], which could physically limit the availability of GSK-3β for phosphorylation.

The main activation process of the cellular energy sensor AMPK has previously been reported to heavily rely on the presence of AXIN in which AXIN knockdown resulted in severely compromised AMPK activation [107]. However, the Western blot analysis in this study revealed that there was no clear correlation between the abundance of AXIN1/2 and the induced activation of AMPK at 48 hours: The untreated cells had strong activation of AMPK even though AXIN1 and AXIN2 were almost absent (Figure 21B, left panel), whereas AMPK activation was attenuated in the treated cells having higher stabilization of AXIN1/2 (Figure 21B, right panel). Together, these findings may indicate that high presence of AXIN may not always be relevant for AMPK activation, especially not for activation during differentiation of human ESCs. On the other hand, it can be speculated that AXIN1/2 may not have been available for the LKB1-mediated AMPK activation process [107] due to an accumulation at other cytoplasmic sites such as the β-catenin destruction complex [56, 91, 143].

Since stimulation of autophagy, by AMPK activation and mTOR signaling inhibition, appears to be important for differentiation and development [10, 13, 14], then factors disrupting this stimulation should have a negative effect on ESC lineage commitment. Indeed, TNKS1/2 inhibition, which notably caused a reduced activation of AMPK concomitantly with reduced attenuation of the AKT/mTOR pathway at 48 hours (Figure 21B, right panel), did efficiently block the differentiation program. These findings raise the possibility that the TNKS-mediated PARsylation of target proteins is important for endodermal differentiation of human ESCs. Furthermore, these observations clearly underline the well-studied interaction between the AMPK pathway and the mTOR pathway [15, 108, 110]: Decreased activation of AMPK was clearly correlated with increased activation of mTOR (Figure 21B, right panel). Moreover, the increased activation of mTOR is followed by an up-regulated activation of AKT (Figure 21B, right panel). This finding concur with previous research showing that mTOR directly activates and phosphorylates AKT at Ser473, thereby enhancing AKT/mTOR signaling [113]. Therefore, TNKS inhibition may not have resulted in downregulated AKT signaling in the treated cells, as it previously has been shown to do in a subtype of cancer cell

lines [123]. In summary, these results demonstrate how TNKS1/2 inhibition also can affect metabolic pathways at the molecular level, not just the WNT pathway, which is consistent with the fact that TNKS1/2 are involved in the regulation of a wide range of cellular processes. However, the exact mechanisms behind the TNKS inhibitor-mediated effects on GSK-3β, AKT/mTOR signaling and the important crosstalk between all these pathways, must further be examined. One approach is to utilize *TNKS1/TNKS2* knockout ESCs. Another is to use esiRNA directed against TNKS1 and 2.

5.2.3 Insufficient effect of the AKT activator SC79 during the differentiation process

Based on the results from the first Western blot analysis showing that the abundance of active and phosphorylated AKT gradually decreased during the differentiation process (Figure 21B, left panel), the next and last step in this study was to assess whether this decrease could be counteracted by utilizing an AKT activator (SC79). This activator has been designed to bind to the plecktrin homology domain of AKT in order to induce a conformational change that facilitates activation and phosphorylation of AKT by upstream kinases [144]. In the study where SC79 was developed, stable HeLa cells exhibited markedly enhanced phosphorylation of Ser473 after being treated with SC79 (11 µM) for 30 minutes [144]. However, in this study, SC79 failed to enhance Ser473 phosphorylation of AKT in the human ESCs during the first 24 hours of the differentiation process, even though higher concentrations (0, 2, 5, 10, 15 µM) of SC79 were used (Figure 22). This insufficient effect of SC79 may be due to intrinsic cell-type-specific differences between the human ESC line H1 and the HeLa cell line used in the study where SC79 was developed.

6 Concluding remarks

This study has provided new insights into the molecular mechanisms behind the WNT and AKT/mTOR signaling pathways in early endodermal differentiation of human ESCs. Interestingly, there is a biphasic regulation of nearly all the proteins, especially the ones involved in the WNT pathway, during the differentiation process, which to our knowledge has not yet been well described. The precise implications of the observed biphasic regulation await further investigation. Furthermore, the changes in the activity of AMPK are clearly inversely related to the changes in the activities of mTOR and AKT throughout the differentiation process. Notably, the activity of AMPK was clearly up-regulated at the end of the process, thus revealing an involvement of catabolic processes during cell fate commitment, at least under the tested conditions. Finally, this study demonstrates the relevance of active TNKS1/2 to maintain both its effect on downstream components and the CHIR99021-mediated stimulation of WNT signaling, which both appear to be crucial for an efficiently endodermal differentiation. Combined, these findings provide a deeper understanding of the molecular principles governing the early differentiation process of ESCs.

References

1. Rippon, H.J. and A.E. Bishop, *Embryonic stem cells.* Cell Proliferation, 2004. **37**(1): p. 23-34.
2. *A conceptual history of modern embryology.* Dev.Biol.(N.Y.1985.), 1991. **7**: p. 1-258.
3. Sui, L., L. Bouwens, and J.K. Mfopou, *Signaling pathways during maintenance and definitive endoderm differentiation of embryonic stem cells.* Int J Dev Biol, 2013. **57**(1): p. 1-12.
4. Sugimura, R. and L. Li, *Noncanonical Wnt signaling in vertebrate development, stem cells, and diseases.* Birth Defects Res.C.Embryo.Today, 2010. **90**(4): p. 243-256.
5. Clevers, H., *Wnt/beta-catenin signaling in development and disease.* Cell, 2006. **127**(3): p. 469-480.
6. Logan, C.Y. and R. Nusse, *The Wnt signaling pathway in development and disease.* Annu.Rev.Cell Dev.Biol., 2004. **20**: p. 781-810.
7. Blauwkamp, T.A., et al., *Endogenous Wnt signalling in human embryonic stem cells generates an equilibrium of distinct lineage-specified progenitors.* Nature communications, 2012. **3**: p. 1070.
8. Nakanishi, M., et al., *Directed induction of anterior and posterior primitive streak by Wnt from embryonic stem cells cultured in a chemically defined serum-free medium.* The FASEB Journal, 2009. **23**(1): p. 114-122.
9. Siller, R., et al., *Small-Molecule-Driven Hepatocyte Differentiation of Human Pluripotent Stem Cells.* Stem Cell Reports, 2015. **4**(5): p. 939-952.
10. Teslaa, T. and M.A. Teitell, *Pluripotent stem cell energy metabolism: an update.* The EMBO journal, 2014: p. e201490446.
11. Ito, K. and T. Suda, *Metabolic requirements for the maintenance of self-renewing stem cells.* Nature reviews. Molecular cell biology, 2014. **15**(4): p. 243-256.
12. Shyh-Chang, N. and George Q. Daley, *Metabolic Switches Linked to Pluripotency and Embryonic Stem Cell Differentiation.* Cell Metabolism. **21**(3): p. 349-350.
13. Mizushima, N. and B. Levine, *Autophagy in mammalian development and differentiation.* Nat Cell Biol, 2010. **12**(9): p. 823-830.
14. Aymard, E., et al., *Autophagy in human keratinocytes: an early step of the differentiation?* Experimental Dermatology, 2011. **20**(3): p. 263-268.
15. Inoki, K., et al., *TSC2 integrates Wnt and energy signals via a coordinated phosphorylation by AMPK and GSK3 to regulate cell growth.* Cell, 2006. **126**(5): p. 955-968.
16. Luckey, C.J., Y. Lu, and J.A. Marto, *Understanding the first steps in embryonic stem cell exit from the pluripotent state.* Transfusion, 2011. **51**(s4): p. 118S-124S.
17. Gadue, P., et al., *Wnt and TGF-β signaling are required for the induction of an in vitro model of primitive streak formation using embryonic stem cells.* Proceedings of the National Academy of Sciences, 2006. **103**(45): p. 16806-16811.
18. Wolpert, L., C. Tickle, and A.M. Arias, *Principles of development*. 2015: Oxford University Press, USA.
19. Boundless, *Boundless Anatomy and Physiology*. Gastrulation. 2015.
20. Merrill, B.J., *Wnt pathway regulation of embryonic stem cell self-renewal.* Cold Spring Harbor perspectives in biology, 2012. **4**(9): p. a007971.
21. De Wert, G. and C. Mummery, *Human embryonic stem cells: research, ethics and policy.* Human reproduction, 2003. **18**(4): p. 672-682.
22. Liu, N., et al., *Molecular mechanisms involved in self-renewal and pluripotency of embryonic stem cells.* Journal of Cellular Physiology, 2007. **211**(2): p. 279-286.

23. Pera, M.F., B. Reubinoff, and A. Trounson, *Human embryonic stem cells.* Journal of Cell Science, 2000. **113**(1): p. 5-10.
24. Justice, M.J., L.D. Siracusa, and A.F. Stewart, *Technical approaches for mouse models of human disease.* Disease Models and Mechanisms, 2011. **4**(3): p. 305-310.
25. Pera, M.F. and A.O. Trounson, *Human embryonic stem cells: prospects for development.* Development, 2004. **131**(22): p. 5515-5525.
26. Murnaghan, I. 2015 [cited 2015 13 Aug]; Available from: http://www.explorestemcells.co.uk/WhyPerformStemCellTransplant.html.
27. Dhar, D. and J. Hsi-En Ho, *Stem cell research policies around the world.* Yale J Biol Med, 2009. **82**(3): p. 113-115.
28. Takahashi, K. and S. Yamanaka, *Induction of pluripotent stem cells from mouse embryonic and adult fibroblast cultures by defined factors.* cell, 2006. **126**(4): p. 663-676.
29. National Institutes of Health, U.S. 2015 Thursday, March 05, 2015. [cited 2015 26 November]; Available from: http://stemcells.nih.gov/info/basics/pages/basics1.aspx.
30. Bilic, J. and J.C.I. Belmonte, *Concise review: Induced pluripotent stem cells versus embryonic stem cells: close enough or yet too far apart?* Stem Cells, 2012. **30**(1): p. 33-41.
31. Zhou, M., et al., *Differentiation of mouse embryonic stem cells into hepatocytes induced by a combination of cytokines and sodium butyrate.* Journal of cellular biochemistry, 2010. **109**(3): p. 606-614.
32. Morey, L., A. Santanach, and L. Di Croce, *Pluripotency and epigenetic factors in mouse embryonic stem cell fate regulation.* Molecular and cellular biology, 2015. **35**(16): p. 2716-2728.
33. Wang, Z., et al., *Distinct Lineage Specification Roles for NANOG, OCT4, and SOX2 in Human Embryonic Stem Cells.* Cell Stem Cell, 2012. **10**(4): p. 440-454.
34. Boyer, L.A., et al., *Core Transcriptional Regulatory Circuitry in Human Embryonic Stem Cells.* Cell, 2005. **122**(6): p. 947-956.
35. Kunath, T., et al., *FGF stimulation of the Erk1/2 signalling cascade triggers transition of pluripotent embryonic stem cells from self-renewal to lineage commitment.* Development, 2007. **134**(16): p. 2895-2902.
36. James, D., et al., *TGFβ/activin/nodal signaling is necessary for the maintenance of pluripotency in human embryonic stem cells.* Development, 2005. **132**(6): p. 1273-1282.
37. Hay, D.C., et al., *Efficient differentiation of hepatocytes from human embryonic stem cells exhibiting markers recapitulating liver development in vivo.* Stem cells, 2008. **26**(4): p. 894-902.
38. Loebel, D.A.F., et al., *Lineage choice and differentiation in mouse embryos and embryonic stem cells.* Developmental Biology, 2003. **264**(1): p. 1-14.
39. Arnold, S.J. and E.J. Robertson, *Making a commitment: cell lineage allocation and axis patterning in the early mouse embryo.* Nat Rev Mol Cell Biol, 2009. **10**(2): p. 91-103.
40. Sokol, S.Y., *Maintaining embryonic stem cell pluripotency with Wnt signaling.* Development, 2011. **138**(20): p. 4341-4350.
41. Borowiak, M., et al., *Small Molecules Efficiently Direct Endodermal Differentiation of Mouse and Human Embryonic Stem Cells.* Cell Stem Cell, 2009. **4**(4): p. 348-358.
42. Dalton, S., *Signaling networks in human pluripotent stem cells.* Current opinion in cell biology, 2013. **25**(2): p. 241-246.
43. Ferrer Tur, R. and M. Duñach i Masjuan, *Pluripotency of embryonic stem cells.* 2014.

44. Ying, Q.-L., et al., *The ground state of embryonic stem cell self-renewal.* Nature, 2008. **453**(7194): p. 519-523.
45. Litwack, G., *Stem Cell Regulators*. Vol. 87. 2011: Academic Press.
46. Rajasekhar, V.K. and M.C. Vemuri, *Regulatory networks in stem cells*. 2009: Springer.
47. Vallier, L., M. Alexander, and R.A. Pedersen, *Activin/Nodal and FGF pathways cooperate to maintain pluripotency of human embryonic stem cells.* Journal of Cell Science, 2005. **118**(19): p. 4495-4509.
48. Lee, M.Y., et al., *Smad, PI3K/Akt, and Wnt-Dependent Signaling Pathways Are Involved in BMP-4-Induced ESC Self-Renewal.* STEM CELLS, 2009. **27**(8): p. 1858-1868.
49. Li, Z. and Y.-G. Chen, *Functions of BMP signaling in embryonic stem cell fate determination.* Experimental Cell Research, 2013. **319**(2): p. 113-119.
50. Xu, R.-H., et al., *Basic FGF and suppression of BMP signaling sustain undifferentiated proliferation of human ES cells.* Nat Meth, 2005. **2**(3): p. 185-190.
51. Vallier, L., et al., *Activin/Nodal signalling maintains pluripotency by controlling Nanog expression.* Development (Cambridge, England), 2009. **136**(8): p. 1339-1349.
52. Yeo, J.-C. and H.-H. Ng, *The transcriptional regulation of pluripotency.* Cell research, 2013. **23**(1): p. 20-32.
53. Eiselleova, L., et al., *A Complex Role for FGF-2 in Self-Renewal, Survival, and Adhesion of Human Embryonic Stem Cells.* Stem Cells, 2009. **27**(8): p. 1847-1857.
54. Singh, Amar M., et al., *Signaling Network Crosstalk in Human Pluripotent Cells: A Smad2/3-Regulated Switch that Controls the Balance between Self-Renewal and Differentiation.* Cell Stem Cell, 2012. **10**(3): p. 312-326.
55. Veeman, M.T., J.D. Axelrod, and R.T. Moon, *A second canon. Functions and mechanisms of beta-catenin-independent Wnt signaling.* Dev.Cell, 2003. **5**(3): p. 367-377.
56. Waaler, J., *Development of specific tankyrase inhibitors for attenuating canonical Wnt/β-catenin signaling*, in *Unit for Cell Signaling, Institute of Microbiology*. 2013, Oslo University Hospital, Rikshospitalet. p. 60.
57. de Jonge, W., *Wnt/β-catenin's regulatory role in embryonic stem cell pluripotency and differentiation.* 2014.
58. Zeng, L., et al., *The mouse Fused locus encodes Axin, an inhibitor of the Wnt signaling pathway that regulates embryonic axis formation.* Cell, 1997. **90**(1): p. 181-192.
59. Perry, W.L., III, et al., *Phenotypic and molecular analysis of a transgenic insertional allele of the mouse Fused locus.* Genetics, 1995. **141**(1): p. 321-332.
60. Miller, J.R. and R.T. Moon, *Signal transduction through beta-catenin and specification of cell fate during embryogenesis.* Genes Dev., 1996. **10**(20): p. 2527-2539.
61. Su, L.K., B. Vogelstein, and K.W. Kinzler, *Association of the APC tumor suppressor protein with catenins.* Science, 1993. **262**(5140): p. 1734-1737.
62. Rubinfeld, B., et al., *Association of the APC gene product with beta-catenin.* Science, 1993. **262**(5140): p. 1731-1734.
63. Kinzler, K.W., et al., *Identification of a gene located at chromosome 5q21 that is mutated in colorectal cancers.* Science, 1991. **251**(4999): p. 1366-1370.
64. Yanagawa, S., et al., *Casein kinase I phosphorylates the Armadillo protein and induces its degradation in Drosophila.* EMBO J., 2002. **21**(7): p. 1733-1742.
65. Amit, S., et al., *Axin-mediated CKI phosphorylation of beta-catenin at Ser 45: a molecular switch for the Wnt pathway.* Genes Dev., 2002. **16**(9): p. 1066-1076.

66. Liu, C., et al., *Control of beta-catenin phosphorylation/degradation by a dual-kinase mechanism.* Cell, 2002. **108**(6): p. 837-847.
67. Yost, C., et al., *The axis-inducing activity, stability, and subcellular distribution of beta-catenin is regulated in Xenopus embryos by glycogen synthase kinase 3.* Genes Dev., 1996. **10**(12): p. 1443-1454.
68. Li, V.S., et al., *Wnt signaling through inhibition of β-catenin degradation in an intact Axin1 complex.* Cell, 2012. **149**(6): p. 1245-1256.
69. Kimelman, D. and W. Xu, *beta-catenin destruction complex: insights and questions from a structural perspective.* Oncogene, 2006. **25**(57): p. 7482-7491.
70. MacDonald, B.T., K. Tamai, and X. He, *Wnt/beta-catenin signaling: components, mechanisms, and diseases.* Dev.Cell, 2009. **17**(1): p. 9-26.
71. Salahshor, S. and J. Woodgett, *The links between axin and carcinogenesis.* Journal of clinical pathology, 2005. **58**(3): p. 225-236.
72. Bernkopf, D.B., M.V. Hadjihannas, and J. Behrens, *Negative-feedback regulation of the Wnt pathway by conductin/axin2 involves insensitivity to upstream signalling.* Journal of Cell Science, 2015. **128**(1): p. 33-39.
73. Kuhl, M., et al., *The Wnt/Ca2+ pathway: a new vertebrate Wnt signaling pathway takes shape.* Trends Genet., 2000. **16**(7): p. 279-283.
74. Rao, T.P. and M. Kuhl, *An updated overview on Wnt signaling pathways: a prelude for more.* Circ.Res., 2010. **106**(12): p. 1798-1806.
75. Zeng, X., et al., *Initiation of Wnt signaling: control of Wnt coreceptor Lrp6 phosphorylation/activation via frizzled, dishevelled and axin functions.* Development, 2008. **135**(2): p. 367-375.
76. Tamai, K., et al., *A mechanism for Wnt coreceptor activation.* Mol.Cell, 2004. **13**(1): p. 149-156.
77. Bilic, J., et al., *Wnt induces LRP6 signalosomes and promotes dishevelled-dependent LRP6 phosphorylation.* Science, 2007. **316**(5831): p. 1619-1622.
78. Davidson, G., et al., *Casein kinase 1 gamma couples Wnt receptor activation to cytoplasmic signal transduction.* Nature, 2005. **438**(7069): p. 867-872.
79. MacDonald, B.T., et al., *Wnt signal amplification via activity, cooperativity, and regulation of multiple intracellular PPPSP motifs in the Wnt co-receptor LRP6.* J.Biol.Chem., 2008. **283**(23): p. 16115-16123.
80. Zeng, X., et al., *A dual-kinase mechanism for Wnt co-receptor phosphorylation and activation.* Nature, 2005. **438**(7069): p. 873-877.
81. Daniels, D.L. and W.I. Weis, *β-catenin directly displaces Groucho/TLE repressors from Tcf/Lef in Wnt-mediated transcription activation.* Nature structural & molecular biology, 2005. **12**(4): p. 364-371.
82. Chatterjee, S.S., et al., *Inhibition of β-catenin–TCF1 interaction delays differentiation of mouse embryonic stem cells.* The Journal of cell biology, 2015. **211**(1): p. 39-51.
83. Cole, M.F., et al., *Tcf3 is an integral component of the core regulatory circuitry of embryonic stem cells.* Genes & development, 2008. **22**(6): p. 746-755.
84. Faunes, F., et al., *A membrane-associated β-catenin/Oct4 complex correlates with ground-state pluripotency in mouse embryonic stem cells.* Development, 2013. **140**(6): p. 1171-1183.
85. Yi, F., et al., *Opposing Effects of Tcf3 and Tcf1 Control Wnt-Stimulation of Embryonic Stem Cell Self Renewal.* Nature cell biology, 2011. **13**(7): p. 762-770.
86. Wu, C.-I., et al., *Function of Wnt/β-catenin in counteracting Tcf3 repression through the Tcf3–β-catenin interaction.* Development, 2012. **139**(12): p. 2118-2129.

87. Takao, Y., T. Yokota, and H. Koide, *β-Catenin up-regulates Nanog expression through interaction with Oct-3/4 in embryonic stem cells.* Biochemical and Biophysical Research Communications, 2007. **353**(3): p. 699-705.
88. Davidson, K.C., et al., *Wnt/β-catenin signaling promotes differentiation, not self-renewal, of human embryonic stem cells and is repressed by Oct4.* Proceedings of the National Academy of Sciences, 2012. **109**(12): p. 4485-4490.
89. Miki, T., S.-y. Yasuda, and M. Kahn, *Wnt/β-catenin signaling in embryonic stem cell self-renewal and somatic cell reprogramming.* Stem Cell Reviews and Reports, 2011. **7**(4): p. 836-846.
90. Wu, Y., et al., *CHIR99021 promotes self-renewal of mouse embryonic stem cells by modulation of protein-encoding gene and long intergenic non-coding RNA expression.* Experimental cell research, 2013. **319**(17): p. 2684-2699.
91. Haikarainen, T., S. Krauss, and L. Lehtiö, *Tankyrases: structure, function and therapeutic implications in cancer.* Current pharmaceutical design, 2014. **20**(41): p. 6472.
92. Huang, S.M., et al., *Tankyrase inhibition stabilizes axin and antagonizes Wnt signalling.* Nature, 2009. **461**(7264): p. 614-620.
93. Waaler, J., et al., *A novel tankyrase inhibitor decreases canonical Wnt signaling in colon carcinoma cells and reduces tumor growth in conditional APC mutant mice.* Cancer research, 2012. **72**(11): p. 2822-2832.
94. Waaler, J., et al., *Novel synthetic antagonists of canonical Wnt signaling inhibit colorectal cancer cell growth.* Cancer Research, 2011. **71**(1): p. 197-205.
95. Hottiger, M.O., et al., *Toward a unified nomenclature for mammalian ADP-ribosyltransferases.* Trends Biochem.Sci., 2010. **35**(4): p. 208-219.
96. Guo, H.-L., et al., *The Axin/TNKS complex interacts with KIF3A and is required for insulin-stimulated GLUT4 translocation.* Cell Research, 2012. **22**(8): p. 1246-1257.
97. Chiang, Y.J., et al., *Tankyrase 1 and tankyrase 2 are essential but redundant for mouse embryonic development.* PloS one, 2008. **3**(7): p. e2639.
98. Zhong, L., et al., *The PARsylation activity of tankyrase in adipose tissue modulates systemic glucose metabolism in mice.* Diabetologia, 2015: p. 1-10.
99. Lau, T., et al., *A novel tankyrase small-molecule inhibitor suppresses APC mutation–driven colorectal tumor growth.* Cancer research, 2013. **73**(10): p. 3132-3144.
100. Voronkov, A., et al., *Structural basis and SAR for G007-LK, a lead stage 1, 2, 4-triazole based specific tankyrase 1/2 inhibitor.* Journal of medicinal chemistry, 2013. **56**(7): p. 3012-3023.
101. Sato, N., et al., *Maintenance of pluripotency in human and mouse embryonic stem cells through activation of Wnt signaling by a pharmacological GSK-3-specific inhibitor.* Nature medicine, 2004. **10**(1): p. 55-63.
102. Berge, D.t., et al., *Wnt signaling mediates self-organization and axis formation in embryoid bodies.* Cell stem cell, 2008. **3**(5): p. 508-518.
103. Engert, S., et al., *Wnt/β-catenin signalling regulates Sox17 expression and is essential for organizer and endoderm formation in the mouse.* Development, 2013. **140**(15): p. 3128-3138.
104. Tahamtani, Y., et al., *Treatment of human embryonic stem cells with different combinations of priming and inducing factors toward definitive endoderm.* Stem cells and development, 2012. **22**(9): p. 1419-1432.
105. Gropper, S. and J. Smith, *Advanced nutrition and human metabolism*. 2012: Cengage Learning.

106. Zhao, J., et al., *AMP-activated protein kinase (AMPK) cross-talks with canonical Wnt signaling via phosphorylation of β-catenin at Ser 552.* Biochemical and biophysical research communications, 2010. **395**(1): p. 146-151.
107. Zhang, Y.-L., et al., *AMP as a low-energy charge signal autonomously initiates assembly of AXIN-AMPK-LKB1 complex for AMPK activation.* Cell metabolism, 2013. **18**(4): p. 546-555.
108. Suzuki, T., et al., *Inhibition of AMPK catabolic action by GSK3.* Molecular cell, 2013. **50**(3): p. 407-419.
109. Kim, I. and Y.-Y. He, *Targeting the AMP-activated protein kinase for cancer prevention and therapy.* Frontiers in Oncology, 2013. **3**.
110. Shimobayashi, M. and M.N. Hall, *Making new contacts: the mTOR network in metabolism and signalling crosstalk.* Nature reviews Molecular cell biology, 2014. **15**(3): p. 155-162.
111. Zhang, C.-S., et al., *The Lysosomal v-ATPase-Ragulator Complex Is a Common Activator for AMPK and mTORC1, Acting as a Switch between Catabolism and Anabolism.* Cell Metabolism, 2014. **20**(3): p. 526-540.
112. Vincent, E.E., et al., *Akt phosphorylation on Thr308 but not on Ser473 correlates with Akt protein kinase activity in human non-small cell lung cancer.* British Journal of Cancer, 2011. **104**(11): p. 1755-1761.
113. Sarbassov, D.D., et al., *Phosphorylation and regulation of Akt/PKB by the rictor-mTOR complex.* Science, 2005. **307**(5712): p. 1098-1101.
114. Inoki, K., et al., *Rheb GTPase is a direct target of TSC2 GAP activity and regulates mTOR signaling.* Genes & Development, 2003. **17**(15): p. 1829-1834.
115. Murakami, M., et al., *mTOR is essential for growth and proliferation in early mouse embryos and embryonic stem cells.* Molecular and cellular biology, 2004. **24**(15): p. 6710-6718.
116. Dufner, A. and G. Thomas, *Ribosomal S6 kinase signaling and the control of translation.* Experimental cell research, 1999. **253**(1): p. 100-109.
117. Jefferies, H.B., et al., *Rapamycin suppresses 5′ TOP mRNA translation through inhibition of p70s6k.* The EMBO journal, 1997. **16**(12): p. 3693-3704.
118. Mak, B.C., et al., *The tuberin-hamartin complex negatively regulates β-catenin signaling activity.* Journal of Biological Chemistry, 2003. **278**(8): p. 5947-5951.
119. Moussaieff, A., et al., *Glycolysis-Mediated Changes in Acetyl-CoA and Histone Acetylation Control the Early Differentiation of Embryonic Stem Cells.* Cell Metabolism, 2015. **21**(3): p. 392-402.
120. Wellen, K.E., et al., *ATP-citrate lyase links cellular metabolism to histone acetylation.* Science, 2009. **324**(5930): p. 1076-1080.
121. Yeung, S., J. Pan, and M.-H. Lee, *Roles of p53, MYC and HIF-1 in regulating glycolysis—the seventh hallmark of cancer.* Cellular and Molecular Life Sciences, 2008. **65**(24): p. 3981-3999.
122. Rennoll, S.A., W.M. Konsavage, and G.S. Yochum, *Nuclear AXIN2 represses MYC gene expression.* Biochemical and biophysical research communications, 2014. **443**(1): p. 217-222.
123. Krauss, S. Oslo University Hospital, Rikshospitalet, Institute of Microbiology: Stefan Krauss lab.
124. Dale, T. 2015: Cardiff University.
125. Feng, G.J., et al., *Conditional disruption of Axin1 leads to development of liver tumors in mice.* Gastroenterology, 2012. **143**(6): p. 1650-1659.
126. Štefková, K., J. Procházková, and J. Pacherník, *Alkaline Phosphatase in Stem Cells.* Stem cells international, 2015. **2015**.

127. Pfaffl, M.W., *Relative quantification.* Real-time PCR, 2006. **63**: p. 63-82.
128. Hoepfner, J., et al., *Biphasic modulation of Wnt signaling supports efficient foregut endoderm formation from human pluripotent stem cells.* Cell biology international, 2016.
129. Chen, E.Y., et al., *Glycogen synthase kinase 3 inhibitors induce the canonical WNT/β-catenin pathway to suppress growth and self-renewal in embryonal rhabdomyosarcoma.* Proceedings of the National Academy of Sciences, 2014. **111**(14): p. 5349-5354.
130. Takahashi, K., M. Murakami, and S. Yamanaka, *Role of the phosphoinositide 3-kinase pathway in mouse embryonic stem (ES) cells.* Biochemical Society Transactions, 2005. **33**(6): p. 1522-1525.
131. Zhou, J., D. Li, and F. Wang, *Assessing the function of mTOR in human embryonic stem cells.* mTOR: Methods and Protocols, 2012: p. 361-372.
132. Sullivan, G.J. 2016.
133. Furue, M.K. 2015.
134. Tanaka, T.S., *Transcriptional heterogeneity in mouse embryonic stem cells.* Reproduction, Fertility and Development, 2008. **21**(1): p. 67-75.
135. Guo, G., et al., *Serum-Based Culture Conditions Provoke Gene Expression Variability in Mouse Embryonic Stem Cells as Revealed by Single-Cell Analysis.* Cell Reports, 2016. **14**(4): p. 956-965.
136. Li, Z., et al., *BMP4 Signaling Acts via Dual-Specificity Phosphatase 9 to Control ERK Activity in Mouse Embryonic Stem Cells.* Cell Stem Cell, 2012. **10**(2): p. 171-182.
137. Ye, S., et al., *Pleiotropy of glycogen synthase kinase-3 inhibition by CHIR99021 promotes self-renewal of embryonic stem cells from refractory mouse strains.* PloS one, 2012. **7**(4): p. e35892.
138. Johansson, H. and S. Simonsson, *Core transcription factors, Oct4, Sox2 and Nanog, individually form complexes with nucleophosmin (Npm1) to control embryonic stem (ES) cell fate determination.* Aging (Albany NY), 2010. **2**(11): p. 815-822.
139. Aymard, E., et al., *Autophagy in human keratinocytes: an early step of the differentiation?* Experimental dermatology, 2011. **20**(3): p. 263-268.
140. Meijer, L., M. Flajolet, and P. Greengard, *Pharmacological inhibitors of glycogen synthase kinase 3.* Trends in Pharmacological Sciences, 2004. **25**(9): p. 471-480.
141. Stolovich, M., et al., *Lithium can relieve translational repression of TOP mRNAs elicited by various blocks along the cell cycle in a glycogen synthase kinase-3-and S6-kinase-independent manner.* Journal of Biological Chemistry, 2005. **280**(7): p. 5336-5342.
142. Case, N., et al., *Mechanical regulation of glycogen synthase kinase 3β (GSK3β) in mesenchymal stem cells is dependent on Akt protein serine 473 phosphorylation via mTORC2 protein.* Journal of Biological Chemistry, 2011. **286**(45): p. 39450-39456.
143. Thorvaldsen, T.E., et al., *Structure, Dynamics, and Functionality of Tankyrase Inhibitor-Induced Degradasomes.* Molecular Cancer Research, 2015. **13**(11): p. 1487-1501.
144. Jo, H., et al., *Small molecule-induced cytosolic activation of protein kinase Akt rescues ischemia-elicited neuronal death.* Proceedings of the National Academy of Sciences, 2012. **109**(26): p. 10581-10586.

Appendix 1: Abbreviations

acetyl-CoA	acetyl coenzyme A
ACTB	β-actin
ADP	adenosine diphosphate
AMP	adenosine monophosphate
AMPK	adenosine monophosphate-activated protein kinase
APC	adenomatous polyposis coli
ART	ADP-ribosyltransferase
ARTD	diphtheria toxin-like ADP-ribosyltransferase
ATP	adenosine triphosphate
AXIN1	axis inhibition protein 1
AXIN2	axis inhibition protein 2
BMPs	bone morphogenetic proteins
cDNA	complementary deoxyribonucleic acid
CK1α	casein kinases 1α
c-MYC	v-Myc avian myelocytomatosis viral oncogene homolog
CRC	colorectal cancer
DAPI	4', 6-diamidino-2-phenylindole
DKO	double knockout
DMEM/F12	Dulbecco's Modified Eagle Medium/Nutrient Mixture F-12
DMSO	dimethyl sulfoxide
DVL	dishevelled
EDTA	ethylenediaminetetraacetic acid
ERK	extracellular signal-regulated kinase
ESCs	embryonic stem cells
FBS	fetal bovine serum
FGFs	fibroblast growth factors
FZD	frizzled
GAP	GTPase-activating protein
GAPDH	glyceraldehyde-3-phosphate dehydrogenase
GDP	guanosine diphosphate
GLUT4	glucose transporter type 4
GSK-3β	glycogen synthase kinase 3β
GTP	guanosine triphosphate
HRP	horseradish peroxidase
Id	inhibitor of differentiation
IMDM	Iscove's Modified Dulbecco's Medium
iPSCs	induced pluripotency stem cells
JAK	Janus kinase
LIF	leukemia inhibitory factor
LKB1	liver kinase B1
LRP5/6	receptor low density lipoprotein receptor-related protein 5/6
MEK	mitogen-activated protein kinase kinase
mRNA	messenger ribonucleic acid
mTOR	mammalian target of rapamycin
mTORC1	mTOR complex 1

NAD^+	nicotinamide adenine dinucleotide
NANOG	nanog homeobox
NGS	normal goat serum
OCT4	octamer-binding transcription factor 4
OXPHOS	oxidative phosphorylation
p70S6K	p70 ribosomal protein S6 kinase
PARP	poly (ADP-ribose) polymerase
PARsylate	poly (ADP-ribose)sylate
PBS	phosphate buffered saline
PI3K	phosphoinositide 3-kinase
PVDF	polyvinylidene difluoride
qRT-PCR	quantitative real-time reverse transcription polymerase chain reaction
RHEB	Ras homolog enriched in brain
RNF146	ring finger protein 146
RPMI	Roswell Park Memorial Institute
RPS6	ribosomal protein S6
RQ	relative quantification
SAM	sterile alpha motif
SDS	sodium dodecyl sulfate
Ser240/244	serine-240/244
Ser2448	serine-2448
Ser473	serine-473
Ser9	serine-9
SOX2	sex-determining region Y, box 2
STAT	signal transducer and activator of transcription
STAT3	signal transducer and activator of transcription 3
TBS	Tris-buffered saline
TCF/LEF	T cell factor/lymphoid enhancer factor
TGF-β	transforming growth factor β
Thr172	threonine-172
Thr308	threonine-308
Thr389	threonine-389
TNKS	tankyrase
TSC	tuberous sclerosis complex
WNT	Wingless-type mouse mammary tumor virus integration site proteins
β-TrCP	β-transducin-repeat-containing protein
$\Delta\Delta C_t$	comparative quantification method

Appendix 2: Materials

Material	Producer	Catalog number
Mouse ESC culture		
Gelatin	Sigma Aldrich	G9391
Dulbecco's Modified Eagle Medium/Nutrient Mixture F-12 (DMEM/F12), GlutaMAX™	Life Technologies	10565018
β-mercaptoethanol	Life Technologies	31350010
Fetal bovine serum (FBS), ES qualified	Life Technologies	16141-079
ESGRO® Leukemia Inhibitory Factor (LIF)	Merck Life Science AS (Millipore)	ESG1106
Penicillin-streptomycin	Sigma Aldrich	P4333
Trypsin - Ethylenediaminetetraacetic acid (EDTA)	Sigma Aldrich	T3924
FBS	Life Technologies	10270-106
CHIR9902	Selleck Chemicals	S2924
PD0325901	Selleck Chemicals	S1036
Human ESC culture		
Essential 8 Medium	Life Technologies	A1517001
Matrigel	Sigma Aldrich	E6909
Advanced Dulbecco's Modified Eagle Medium/Ham's F-12 (DMEM-F12)	Life Technologies	12634028
EDTA	Life Technologies	15575-020
Alkaline phosphatase staining		
Alkaline Phosphatase Staining Kit II	Stemgent	00-0055

Immunofluorescence		
Dulbecco's PBS (calcium/magnesium free)	Life Technologies	14190
Methanol	VWR	20903.368
Normal goat serum (NGS)	Life Technologies	PCN5000
Tween 20	Sigma Aldrich	P7949
OCT4 Antibody	Stemgent	09-0023
NANOG Antibody	Stemgent	09-0020
SOX2 Antibody	Stemgent	09-0024
Alexafluor 488 anti rabbit	Life Technologies	A21206
Alexafluor 594 anti rabbit	Life Technologies	A21207
Fluoroshield with DAPI	Sigma Aldrich	F6057
Differentiation materials for mouse ESCs		
Knockout Dulbecco's Modified Eagle Medium (DMEM)	Life Technologies	10829018
Iscove's Modified Dulbecco's Medium (IMDM)	Life Technologies	12440053
Roswell Park Memorial Institute (RPMI) Medium 1640, GlutaMAX^{TM}	Life Technologies	61870
mESF Basal Medium	Wako Pure Chemical Industries, Ltd	136-17805
Insulin from bovine pancreas	Sigma Aldrich	I5599
Apo-transferrin human	Sigma Aldrich	T2252
2-mercaptoethanol	Life Technologies	31350010
Ethanolamine	Sigma Aldrich	E0135
Sodium selenite	Sigma Aldrich	S9133
Laminin	Sigma Aldrich	11243217001

Recombinant mouse WNT3A	R&D Systems Europe LTD.	1324-WN-010
BSA	Europa Bioproducts Ltd	EQBAC61
EDTA	Life Technologies	15575-020
Differentiation materials for human ESCs		
RPMI Medium 1640, GlutaMAX™	Life Technologies	61870
B-27 supplement with insulin	Life Technologies	17504-044
CHIR99021	Stemgent	04-0004-10
G007-LK	ChemRoyal Inc.	
SC 79	R&D Systems	4635
Dimethyl sulfoxide (DMSO)	Sigma Aldrich	D8418
qRT-PCR materials		
GenEluteTM Mammalian Total RNA Miniprep Kit	Sigma Aldrich	RTN350
High-Capacity cDNA Reverse Transcription kit	Life technologies	4368813
TaqMan Gene Expression Mastermix	Life technologies	4369510
SDS-PAGE and Western blotting		
NP40 Cell Lysis Buffer	Life Technologies	FNN0021
Protease Inhibitor Cocktail Tablets	Roche Applied Science	4693124001
Bradford Assay	Bio-Rad	500-0205
SDS loading buffer (4X)		
Glycerol	Sigma Aldrich	G5516
Sodium dodecyl sulfate (SDS)	Sigma Aldrich	L3771
Bromophenol blue sodium salt	Sigma Aldrich	B5525
β-merkaptoethanol (2-merkaptoethanol)	AppliChem	A1108,0100

Sodium chloride (NaCl)	Sigma Aldrich	S3014
Tris hydrochloride (HCl)	Sigma Aldrich	RES3098T
EDTA	Sigma Aldrich	431788
Transfer buffer		
Trizma-base	Sigma Aldrich	T1503
Glysine	Sigma Aldrich	G7126
Nu-PAGE® Tris-Acetate SDS running buffer 20X	Life Technologies	LA0041
Nu-PAGE® MOPS SDS running buffer 20X	Life Technologies	NP0001
Nu-PAGE® Novex® 4-12% Bis-Tris Protein gels, 1.0 mm, 10 well	Life Technologies	EA0375BOX
Nu-PAGE® Novex® 3-8% Tris-Acetate Protein gels, 1.0 mm, 10 well	Life Technologies	NP0321BOX
Nonfat dried milk	AppliChem	A0830,0500
Tris buffered saline (TBS) tablets	Medicago	09-7510-100
Kit ECL Prime Western Blotting Detection Reagent	GE Healthcare Amersham	RPN2236
Ladders		
PageRuler Prestained Protein Ladder	Thermo Fisher Scientific	26616
Primary antibodies		
Rabbit IgG anti-Tankyrase-½	Santa Cruz Biotechnology, INC.	sc-8337
Rabbit IgG anti-AXIN1	Cell Signaling	2087
Rabbit IgG anti-AXIN2	Cell Signaling	2151
Rabbit IgG anti- non-phopho (active) β-catenin	Cell Signaling	8814
Mouse IgG anti-β-catenin (total)	BD Transduction Laboratories™	610153
Rabbit IgG anti-phospho-GSK3β (Ser9)	Cell Signaling	9323S

Rabbit IgG anti-GSK3β (total)	Cell Signaling	9315S
Rabbit IgG anti-phospho-AMPKα (Thr172)	Cell Signaling	2535
Mouse IgG anti-AMPKα	Cell Signaling	2793S
Rabbit IgG anti-phospho-AKT (Ser473)	Cell Signaling	4060S
Rabbit IgG anti-AKT (total)	Cell Signaling	9272S
Rabbit IgG anti-phospho-mTOR (Ser2448)	Cell Signaling	2971
Rabbit IgG anti-mTOR (total)	Cell Signaling	2972
Rabbit IgG anti-phospho-p70 S6 kinase	Cell Signaling	9205S
Rabbit IgG anti-p70S6K (total)	Cell Signaling	9202
Rabbit IgG anti-phospho-RPS6 (Ser240/244)	Cell Signaling	2215
Rabbit IgG anti-RPS6 (total)	Cell Signaling	2217
Rabbit IgG anti-ACTIN	Sigma Aldrich	A2066
Secondary antibodies		
Donkey anti-mouse IgG-horseradish peroxide (HRP)	Santa Cruz Biotechnology	sc-2314
Donkey anti-rabbit IgG-HRP	Santa Cruz Biotechnology	sc-2313

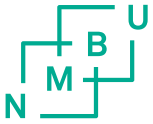

Norges miljø- og biovitenskapelig universitet
Noregs miljø- og biovitskapelege universitet
Norwegian University of Life Sciences

Postboks 5003
NO-1432 Ås
Norway